Dynamics and control at feedback vertex sets. I: Informative and determining nodes in regulatory networks

Bernold Fiedler*
Atsushi Mochizuki**
Gen Kurosawa**
Daisuke Saito**

March 30, 2013

*Fachbereich Mathematik und Informatik
Institut für Mathematik
Arnimallee 3,
D-14195 Berlin, Germany

**Theoretical Biology Laboratory
RIKEN
2-1 Hirosawa
Wako 351-0198, Japan

Abstract

We consider systems of differential equations which model complex regulatory networks by a graph structure of dependencies. We show that the concepts of informative nodes (Mochizuki; see [MoSa10]) and determining nodes (Foias and Temam; see [FoTe84]) coincide with the notion of feedback vertex sets from graph theory.

As a result we can determine the long-time dynamics of the entire network from observations on only a feedback vertex set. We also indicate how open loop control at a feedback vertex set, only, forces the remaining network to stably follow prescribed stable or unstable trajectories.

We present three examples of biological networks which motivated this work: a specific gene regulatory network of ascidian cell differentiation [Im&al06], a signal transduction network involving the epidermal growth factor in mammalian cells [Oda05], and a mammalian gene regulatory network of circadian rhythms [Mi09]. In each example the required observation set is much smaller than the entire network. For further details on biological aspects see the companion paper [Mo&al13].

The mathematical scope of our approach is not limited to biology. Therefore we also include many further examples to illustrate and discuss the broader mathematical aspects.

1 Introduction

Motivated by the dynamics of gene regulatory and signal transduction networks we study nonautonomous nonlinear systems of ordinary differential equations of the form

$$\dot{z}_k = F_k(t, z_k, z_{I_k}), \tag{1.1}$$

$k = 1, \ldots, N$. Here $I_k \subseteq \{1, \ldots, N\}$ are given subsets. For any subset $K \subseteq \{1, \ldots, N\}$, the vector

$$z_K := (z_k)_{k \in K} = P_K z \in \mathbb{R}^{|K|} \tag{1.2}$$

denotes the projection P_K of $z = (z_1, \ldots, z_N) \in \mathbb{R}^N$ to those components z_k with index k in the index set K. For example $z_{\{k\}} := z_k$. As an important special case, also, we will frequently consider the autonomous variant

$$\dot{z}_k = F_k(z_k, z_{I_k}), \tag{1.3}$$

where the nonlinearities do not depend on time t, explicitly. We call such ODE systems (1.1) or (1.3) *regulatory networks*.

We consider the ODE (1.1) as a system given on a *directed graph* (di-graph) Γ with vertices $\{1, \ldots, N\}$. The directed edges of Γ, from vertex i to vertex k, are given precisely by the ordered vertex pairs (i, k) with $i \in I_k$. In other words, the input set I_k defines the predecessors i of vertex k in the oriented graph Γ. In view of ODE (1.1) we also call $i \in I_k$ the *inputs* of k. We explicitly admit the possibility of *self-loops* $k \in I_k$, i.e. directed edges from k back to k itself. For a first example see the *Frobenius graph* of Figure 1.

Throughout the paper we fix the following assumptions. Let the nonlinearities F_k and the z-Jacobians $F_{k,z}$ be continuous, i.e. F_k, $F_{k,z} \in C^0$. Moreover let the ODE (1.1) be *dissipative*, i.e. assume that there exists a large positive constant C such that for any initial condition $z(0) = z_0 \in \mathbb{R}^N$ of (1.1) there exists a positive time t_0 such that $|z(t)| \leq C$, for all $t \geq t_0$. In other words, any solution $z(t)$ of (1.1) eventually enters a Euclidean ball around the origin, of sufficiently large fixed radius C. In particular solutions exist globally in forward time.

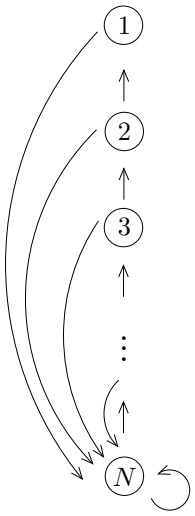

Figure 1: A Frobenius di-graph with N vertices and $2N-1$ edges. Directed edges run from vertex $k+1$ to $k=1,\ldots,N-1$ and from all vertices to N. Note the additional self-loop at vertex N.

An explicit sufficient (but not necessary) condition for dissipativity, for example, requires

$$\sum_{k=1}^{N} z_k F(t, z_k, z_{I_k}) < 0 \tag{1.4}$$

for all $z \in \mathbb{R}^N$ such that $|z| \geq C$.

Our final and crucial assumption is a *decay condition* of the form

$$\partial_1 F_k(t, z_k, z_{I_k}) < 0\,, \tag{1.5}$$

for all $t \geq 0$, $k = 1,\ldots,N$ and bounded $z \in \mathbb{R}^N$. Here ∂_1 indicates the partial derivative with respect to the first z-argument z_k of F_k.

At first sight, the decay condition (1.5) seems to require any self-feedback from vertex k to itself to be negative. Indeed this is the case if the set I_k of predecessors of vertex k does not contain k itself, i.e. $k \notin I_k$. Equivalently, this is the case if the graph Γ of the regulatory network is loop-free, i.e.

Γ does not contain any vertex k with a self-loop. For example the decay condition (1.5) is satisfied, without any self-loops, for networks of the special form $F_k(t, z_k, z_{I_k}) = f_k(t, z_{I_k}) - d_k(t)z_k$, where a positive dilution or decay rate d_k is the only self-feedback of vertex k to itself; see example (8.7) below. More general net-negative self-feedbacks are accommodated just as well, in absence of self-loops.

Self-loops $k \in I_k$, on the other hand, entirely circumvent the decay condition (1.5) to take any effect at all. Indeed, suppose the nonlinearity F_k does not satisfy assumption (1.5) at all. Then, at the expense of including a self-loop via $\widetilde{I}_k := I_k \cup \{k\}$, we may always redefine F_k to be replaced by

$$\widetilde{F}_k(t, \zeta_k, z_{\widetilde{I}_k}) := F_k(t, z_k, z_{I_k}) + z_k - \zeta_k \,. \tag{1.6}$$

In other words, $\widetilde{F}_k$ depends on a new artificial variable ζ_k, in addition to z_{I_k} and z_k in $z_{\widetilde{I}_k} = (z_{I_k}, z_k)$. Evaluating the network ODE (1.1) with $\widetilde{F}_k, \widetilde{I}_k$ replacing F_k, I_k, of course, we have to insert $\zeta_k := z_k$ and the ODE (1.1) remains unchanged – albeit with arbitrary nonmonotone dependence on z_k. Therefore the unaltered ODE structure (1.1), with $\widetilde{I}_k$ instead of I_k and $\widetilde{F}_k$ instead of F_k, always satisfies assumption (1.5) even if F_k itself did not. Summarizing self-loops in the regulatory network graph Γ may indicate a net-positive self-feedback, and should be used in such cases, only.

To study the large time asymptotics of ODE systems

$$\dot{z} = F(t, z) \,, \tag{1.7}$$

$z \in \mathbb{R}^N$ via information $z_I(t)$ on a potentially very small subset $I \subseteq \{1, \dots, N\}$ we introduce the concept of determining nodes. This concept was first considered by Foias and Temam in the technically demanding PDE context of the Navier-Stokes equations for fluid flows; see [FoTe84]. Their emphasis was on a reduction of the asymptotic dynamics from infinite to finite dimensional observations, essentially via spectral gap properties of the linear Stokes operator. Our emphasis here is on a reduction from large networks to potentially very few observations, via graph theoretic properties of the network.

Definition 1.1. *We call a subset I of the vertex set $\{1, \dots, N\}$ a set of* ***determining nodes****, if*

$$\widetilde{z}(t) - z(t) \underset{t \to +\infty}{\longrightarrow} 0 \tag{1.8}$$

holds, for any two solutions $z(t), \widetilde{z}(t)$ of the nonautonomous ODE system (1.7) such that

$$\widetilde{z}_I(t) - z_I(t) \underset{t\to+\infty}{\longrightarrow} 0\,. \tag{1.9}$$

In suitable coordinates we may replace the coordinate projection P_I involved in (1.8), (1.9) by any other projection, of course. In the more specific context of regulatory networks (1.1) on a di-graph Γ, however, we may interpret the determining nodes I as vertices directly and conclude that observations of the determining nodes (1.9) alone are sufficient to determine the large time dynamics (1.8) of the entire network. It is therefore an important task to identify determining node sets I which are, both, as small and as experimentally accessible as possible. We will show below how to identify determining node sets I based on the structure of the di-graph Γ, only.

A *di-cycle* (directed cycle) in a di-graph Γ is an alternating sequence of vertices and edges, traversed in the prescribed orientation, such that the first and last vertex coincide. Self-loops are explicitly allowed. A di-graph Γ without di-cycles is called *acyclic*.

Definition 1.2. *A **feedback vertex set** of a di-graph Γ is a possibly empty subset I of vertices such that the di-graph $\Gamma\setminus I$ is acyclic. Here $\Gamma\setminus I$ denotes the resulting di-graph when all vertices of I are removed from Γ, along with all edges from or towards those vertices.*

As a trivial example note that a di-graph is acyclic if and only if it possesses an empty feedback vertex set. As a second example consider the Frobenius di-graph Γ of Figure 1. Since the vertex $k = N$ possesses a self-loop, any feedback vertex set I must contain N. Conversely, $I = \{N\}$ is a feedback vertex set. Indeed the remaining di-graph $\Gamma\setminus\{N\}$ is given by the acyclic linear chain $N-1 \to \ldots \to 2 \to 1$. Therefore $I = \{N\}$ is the unique minimal feedback vertex set of Γ. In general, however, minimal feedback vertex sets need not be unique. A simple example is the graph of two vertices 1,2 with directed edges from 1 to 2 and from 2 to 1; see also section 5.3.

The problem of finding a minimal feedback vertex set for di-graphs is known to be NP-complete [Ka75]. Moderately cumbersome as the the task to find a minimal feedback vertex set may be, however, it is equivalent to finding a smallest possible set of determining nodes which work for all nonlinearities of

the regulatory network (1.1). This is our first main result, proved in sections 3 and 6 below.

Theorem 1.3. *Consider a nonautonomous regulatory* ODE *network (1.1) with dissipative nonlinearities F_k, and associated di-graph Γ. We also assume F_k, $D_z F_k$ to be continuous. Moreover F_k satisfies the uniform decay condition (1.5).*

Then a possibly empty subset $I \subseteq \{1, \ldots, N\}$ of vertices of Γ is a set of determining nodes for the dynamics of (1.1) and for all choices of nonlinearities F_k if and only if I is a feedback vertex set of the di-graph Γ.

Our second main result shows how the dynamics $z_I(t)$ on a feedback vertex set I faithfully represents the full dynamics of any uniformly bounded solution $z(t)$, for all $t \in \mathbb{R}$, i.e. for all forward and backward time. In particular this includes all steady states, periodic and quasiperiodic solutions and all bounded chaotic trajectories. For simplicity of presentation we restrict to autonomous ODEs, i.e. to regulatory networks

$$\dot{z} = F(z) \tag{1.10}$$

with nonlinearities $F_k(t, z_k, z_{I_k}) = F_k(z_k, z_{I_k})$ which do not depend on time t explicitly. The appropriate concept here is the global attractor.

Definition 1.4. *Assume an autonomous ODE (1.10) to be dissipative, e.g. because the C^1-nonlinearity $F = (F_1, \ldots, F_N)$ satisfies condition (1.4). Then the set*

$$\mathcal{A} := \{z(0) \in \mathbb{R}^N \mid \sup_{t \in \mathbb{R}} |z(t)| < \infty\} \tag{1.11}$$

of initial conditions of uniformly bounded solutions $z(t)$ is called the ***global attractor*** *of (1.6).*

Again, global attractors are a PDE concept first studied in the context of two-dimensional Navier-Stokes fluid flows [La72]. Meanwhile this concept has attracted a lot of attention; see for example the monographs [Ha88, Te88, La91, BaVi92, Ed&al94, ChVi02, Ha&al02, Ra02, SeYo02] and the references there. For our purposes we briefly recall these results, adapted to

our ODE context and justify the name of "global attractor". We begin with the concept of the ω-limit set

$$\omega(z(0)) := \{z_\infty \in \mathbb{R}^N \,\big|\, z_\infty = \lim z(t_n), \text{ for some } t_n \to \infty\} \tag{1.12}$$

of an initial datum $z(0)$. Similarly, we can define the ω-limit set of any subset $B \subseteq \mathbb{R}^N$ via sequences of initial data $z^n(0) \in B$ as

$$\omega(B) := \{z_\infty \in \mathbb{R}^N | z_\infty = \lim\, z^n(t_n), \text{ for } t_n \to \infty,\, z^n(0) \in B\}\,. \tag{1.13}$$

We say that a set A *attracts* a set B, if $\omega(B) \subseteq A$. We say that a set A is *invariant* if $z(0) \in A$ implies $z(t) \in A$, for all positive and negative $t \in \mathbb{R}$. By construction, for example, the above ω-limit sets are invariant. The following characterization of global attractors can be found in [Ha88], for example.

Proposition 1.5. *Assume the autonomous ODE (1.10) is dissipative. Then the global attractor $\mathcal{A} \subseteq \mathbb{R}^N$ of definition 1.4 has the following properties:*

(i) *$\mathcal{A}$ is nonempty, compact and invariant;*

(ii) *$\mathcal{A}$ is the smallest set which attracts all bounded sets;*

(iii) *$\mathcal{A}$ is the largest set which is, both, compact and invariant.*

Since we are in $\mathbb{R}^N$, here, compactness of $\mathcal{A}$ is equivalent to $\mathcal{A}$ being bounded and closed.

We can now formulate our second main result which shows that observations of history time tracks $z_I(t)$ at the determining nodes alone suffice to determine and reconstruct the full dynamics on the global attractor. Let $\mathbb{R}_-$ denote the set of nonpositive real numbers $t \leq 0$. Let BC^2 denote the bounded functions $t \mapsto z(t)$, $t \in \mathbb{R}_-$, with uniformly bounded first and second derivatives, endowed with the compact-open topology of uniform C^2-convergence on bounded subsets of $t \in \mathbb{R}_-$.

Theorem 1.6. *Consider an autonomous regulatory ODE network (1.3) with dissipative C^1-nonlinearities F_k, decay condition (1.4), associated di-graph Γ, feedback vertex set I, and global attractor $\mathcal{A}$.*

Then the continuous projection

$$\begin{aligned} \mathcal{P}_I : \mathcal{A} &\to BC^2(\mathbb{R}_-, \mathbb{R}^{|I|}) \\ z(0) &\mapsto z_I(\cdot) \end{aligned} \tag{1.14}$$

is injective, i.e. one-to-one.

In other words, there is a unique inverse

$$\mathcal{P}_I^{-1}: \quad BC^2(\mathbb{R}_-, \mathbb{R}^{|I|}) \supseteq \text{Range } \mathcal{P}_I \longrightarrow \mathcal{A} \tag{1.15}$$

which reconstructs the full initial condition

$$\mathcal{P}_I^{-1} z_I(\cdot) = z(0) \in \mathcal{A} \tag{1.16}$$

from any history time track $t \mapsto z_I(t)$, $t \in \mathbb{R}_-$, on the feedback vertex set I. A fortiori, this determines any trajectory $t \mapsto z(t)$, $t \in \mathbb{R}$ in the global attractor $\mathcal{A}$ uniquely, from any given history time track $z_I(t)$, $t \in \mathbb{R}_-$, restricted to the feedback vertex set I and to the history $t \leq 0$ of the initial datum $z(0)$ under consideration.

As formulated, theorem 1.6 seems to refer to the history time tracks $t \mapsto z(t)$, $t \in \mathbb{R}_-$, on the global attractor $\mathcal{A}$, rather than experimentally available forward time tracks for $t > 0$. The global attractor $\mathcal{A}$ itself, however, is constructed as a limit $\omega(B)$ in forward time $t_n \to \infty$. Therefore the history time tracks on the global attractor $\mathcal{A}$ can be thought of as being well approximated by measurements of forward time tracks, in any experimental setting.

For the proper interpretation of theorem 1.6 for acyclic regulatory networks Γ, i.e. for the case of empty feedback vertex sets I, see example 5.1 below.

The remaining sections are organized as follows. In section 2 we show that the notion of a feedback vertex set coincides with the notion of a set of informative nodes as introduced by Mochizuki and Saito in [MoSa10]; see corollary 2.4. Based on this equivalence we can pass from the feedback vertices to determining nodes, in section 3, and prove the if-part of feedback vertex theorem 1.3 on their equivalence.

Section 4 is devoted to the proof of theorem 1.6 on the unique reconstruction of global attractors from the history time tracks on the feedback vertex set. As a corollary we recover the results on steady states of [Mo08, MoSa10] in corollary 4.1. We illustrate both results with some mathematical examples, in section 5. In particular we discuss the Frobenius di-graph of Figure 1 with linear flow in some detail. Based on such examples we prove the converse only-if-part of feedback vertex theorem 1.3 in section 6. Three biological

examples are addressed in section 7. See also the companion paper [Mo&al13] for a more thorough presentation of biological aspects. We conclude in section 8 with a discussion of our results – and a string of caveats.

Acknowledgement. The first two authors gratefully acknowledge pleasant excesses of mutual hospitality during very enjoyable working visits. We are also indebted to Sze-Bi Hsu and NCTS Taiwan for generous hospitality and helpful comments. The relation with determining nodes was suggested by Abderrahim Azouani. Hiroshi Kokubu, Hiroe Oka, Genevieve Raugel and her insightful referee have greatly assisted with valuable further suggestions. Skillful and very patient typesetting was gracefully achieved by Margrit Barrett and Ulrike Geiger. This work was generously supported by the Deutsche Forschungsgemeinschaft, SFB 910 "Control of Self-Organizing Nonlinear Systems".

2 Feedback vertices, infomative nodes, and labeling order

In this section we study the di-graph Γ associated with the regulatory network (1.1). In definition 1.2 we have introduced feedback vertex sets I of Γ: upon removal of I the remaining di-graph $\Gamma \setminus I$ becomes acyclic. In definition 2.1 below we introduce informative sets, as developed by Mochizuki and Saito in their study [MoSa10] of steady states of gene regulatory networks. Lemma 2.2 provides a convenient labeling order of the vertices $1, \dots, N$ of regulatory networks (1.1) with informative set I. Our proofs of theorems 1.3 and 1.6 will be based on this labeling order. As an immediate consequence we obtain the equivalence of the notions of feedback vertex sets and informative sets, in Corollary 2.4.

Definition 2.1.

*(i) A possibly empty subset $I \subseteq \{1, \dots, N\}$ of the vertex set of a di-graph Γ is called **informative**, if for any nonzero $\zeta \in \mathbb{R}^N$ with $\zeta_I = 0$ there exists a vertex n such that $\zeta_n \neq 0$ but $\zeta_{I_n} = 0$.*

(ii) Equivalently, for any distinct $z, \widetilde{z} \in \mathbb{R}^N$ which coincide on I there exists a vertex n such that $z, \widetilde{z}$ coincide on the predecessors I_n of n, but $\widetilde{z}_n \neq z_n$.

The equivalence claim of definition 2.1 is obvious. We write $\zeta := \widetilde{z} - z$ to prove (i) implies (ii). We choose $z := 0$, $\widetilde{z} := \zeta$ for the reverse direction. The steady state analysis of regulatory networks (1.1) in [MoSa10] was based on the second variant.

Lemma 2.2. *Let $\varnothing \subseteq I \subseteq \{1, \ldots, N\}$ be informative for the di-graph Γ. We label $I = \{N' + 1, \ldots, N\}$ with $N' := N - |I|$ in case I is nonempty.*

Then there exists an ordered labeling of the vertices $J := \{1, \ldots, N'\}$ of the remaining di-graph $\Gamma \backslash I$, upon removal of I, such that

$$I_{n'} \subseteq I \cup \{1, \ldots, n' - 1\} \tag{2.1}$$

holds for all predecessor sets $I_{n'}$ of the remaining vertices $n' \in J$.

Conversely, $I = \{N' + 1, \ldots, N\}$ is informative for Γ if (2.1) holds for all $1 \leq n' \leq N'$.

Proof.
We characterize the informative set I by definition 2.1(i). We skip the trivial case $|I| = N$, $N' = 0$ and proceed by induction over $n' \geq 1$.

For $n' = 1$ we choose $\zeta := 1_J \neq 0$ to vanish on I and have components $\zeta_j = 1$ for all $j \in J = \{1, \ldots, N'\}$. Because I is informative there exists n with $\zeta_{I_n} = 0$ and $\zeta_n \neq 0$. By construction $I_n \subseteq I$ and $n \in J$. Relabeling this n as 1 shows (2.1) for $n' = 1$.

To show the induction step suppose we have shown claim (2.1) up to but not including some $1 < n' \leq N'$. To show (2.1) for n' we choose $\zeta := 1_{\{n', \ldots, N'\}}$ to be the nonzero indicator of the remaining vertices $n', \ldots, N'$ in J. Again because I is informative, there exists n with $\zeta_{I_n} = 0$ and $\zeta_n \neq 0$. By construction $I_n \subseteq I \cup \{1, \ldots, n' - 1\}$ and $n' \leq n \leq N'$. Relabeling this n as n' shows (2.1). This completes the induction.

Conversely suppose (2.1) holds. To show $I = \{N' + 1, \ldots, N\}$ is informative let $\zeta \neq 0$ vanish on I. Choose $1 \leq n \leq N'$ minimal such that $\zeta_n \neq 0$. Then $\zeta_{I \cup \{1, \ldots, n-1\}} = 0$ by definition of n. But (2.1) with $n' := n$ implies $I_n \subseteq I \cup \{1, \ldots, n - 1\}$. Therefore $\zeta_{I_n} = 0$, and the converse claim is also proved. $\square$

See Figure 2 for an illustration of lemma 2.2 with informative set $I = \{N\}$. By comparison with the Frobenius graph of Figure 1 note the reversed or-

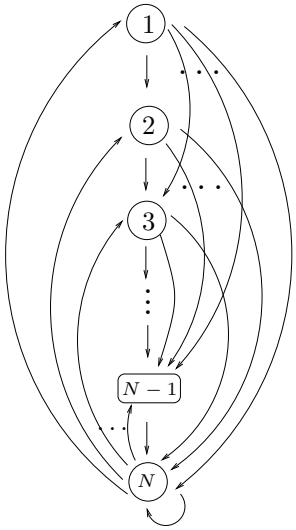

Figure 2: The maximal di-graph Γ with informative set $I = \{N\}$. Predecessor sets $I_{n'}$ are $I \cup \{1, \ldots, n' - 1\}$ for $1 \leq n' \leq N' = N - 1$, i.e. for $n' \notin I$. The predecessor set I_N of the single informative node N is all of $\{1, \ldots, N\}$. In other words, the oriented edge $i \to j$ exists unless $1 \leq j \leq i \leq N - 1$. Some of the indicated edges may be absent in other di-graphs Γ with a single informative node.

dering of the complementary vertices $1, \ldots, N-1$ and the omitted arrows there.
Labeling orders are not unique, in general. Reverting some, but not all, arrows in the vertical chain $N-1 \to \ldots \to 2 \to 1$ of Figure 1, for example, offers several choices of top vertices $n' = 1$ without predecessors.

To prove equivalence of informative sets and feedback vertex sets we show next that feedback vertex sets I are characterized by the same labeling order (2.1) as informative sets are.

Lemma 2.3. *A possibly empty subset $I \subseteq \{1, \ldots, N\}$ of the vertex set of a di-graph Γ is a feedback vertex set if, and only if, the vertices $n' \in J := \{1, \ldots, N'\}$ of the remaining di-graph $\Gamma \setminus I$ possess an ordered labeling such that (2.1) holds.*

Proof.
By definition 1.2 the set I is a feedback vertex set if and only if $\Gamma \setminus I$ is acyclic. Acyclicity, in turn, is equivalent to the edge orientation of $\Gamma \setminus I$ defining a strict partial order $\prec$ on the vertices J. Here we define $j_1 \prec j_2$ on J, if $j_1 \neq j_2$ and there exists an oriented path in $\Gamma \setminus I$ from j_1 to j_2.

Since J is finite, we can extend the strict partial order $\prec$ to a strict total order on J. Labeling the vertices of J in ascending strict total order proves (2.1), for any feedback vertex set I.

Conversely, (2.1) defines a strict total order on J. In particular $\Gamma \setminus I$ is acyclic and I is a feedback vertex set. This proves the lemma. $\square$

Corollary 2.4. *A possibly empty subset $I \subseteq \{1, \ldots, N\}$ of the vertex set of a di-graph Γ is a feedback vertex set if, and only if, it is informative.*

Proof.
By lemmas 2.2 and 2.3 the informative and the feedback vertex property of I are each equivalent to the labeling order (2.1) on $\Gamma \setminus I$. $\square$

As a curiosity we observe invariance of the feedback vertex sets under orientation reversal. Indeed let $\overline{\Gamma}$ denote the di-graph Γ with reversed orientation of all edges. This preserves all cycles, albeit with reversed orientation, and therefore preserves any feedback vertex sets. Invariance of informative sets

ensues by lemma 2.3. This informative invariance is less intuitive because the dependence hierarchy of predecessor $\longrightarrow$ successor is reversed in $\overline{\Gamma}$.

3 From feedback vertices to determining nodes

In this section we prove the if-part of theorem 1.3 on determining nodes of nonautonomous regulatory networks, as formulated in lemma 3.2 below. For preparation we study the linear variant of the gene regulatory network (1.1) in lemma 3.1.

To be specific consider the linear nonautonomous regulatory network

$$\dot{w}_k(t) = -a_k(t)w_k + b_k^T(t)w_{I_k}(t) \tag{3.1}$$

on the di-graph Γ with continuous nonautonomous coefficients $a_k(t) \in \mathbb{R}$, $b_k(t) \in \mathbb{R}^{|I_k|}$. We also assume uniform bounds

$$0 < a_0 \leq a_k(t); \qquad |b_k(t)| \leq b_0 \tag{3.2}$$

for all $1 \leq k \leq N$ and all $t \geq 0$.

Lemma 3.1. *Let (3.1), (3.2) hold and let I be a feedback vertex set of the di-graph Γ. Assume convergence*

$$w_I(t) \longrightarrow 0, \tag{3.3}$$

for $t \to +\infty$, i.e. $w_k(t) \longrightarrow 0$, for all $k \in I$.

Then we also have convergence

$$w_J(t) \longrightarrow 0, \tag{3.4}$$

for $t \to +\infty$, i.e. $w_k(t) \longrightarrow 0$ for all k in the complementary set J of vertices in the remaining di-graph $\Gamma \setminus I$.

In short, $w_I(t) \longrightarrow 0$ implies $w(t) \longrightarrow 0$.

Proof.
Following lemmas 3.2 and 3.3 we relabel the vertices of Γ such that $J = \{1, \ldots, N'\}$, $I = \{N' + 1, \ldots, N\}$ and

$$I_{n'} \subseteq I \cup \{1, \ldots, n' - 1\} \tag{3.5}$$

by labeling order (2.1). We prove decay (3.4) by induction over k.

Suppose claim (3.4) has been proved for all $k \in \{1, \dots, n'-1\}$. To show (3.4) for $k = n'$ we use variations-of-constants in ODE (3.1) together with estimates (3.2) and the induction hypothesis on (3.4) to estimate

$$
\begin{aligned}
|w_{n'}(t)| \leq & \left(\exp\left(-\int_0^t a_n(s)ds \right) |w_{n'}(0)| + \right. \\
& \left. + \sum_{j \in I_{n'}} \int_0^t \exp\left(-\int_s^t a_{n'}(\sigma)d\sigma \right) \cdot |b_j(s)| \cdot |w_j(s)| ds \right) \\
\leq & \left(e^{-a_0 t}|w_{n'}(0)| + \sum_{j \in I_{n'}} \int_0^t \exp\left(-a_0(t-s)\right) b_0 |w_j(s)| ds \right) \\
\to & \quad 0
\end{aligned}
\tag{3.6}
$$

for $t \to +\infty$. Indeed convergence is exponential in the first term. The integral terms equal

$$
b_0 \int_0^t e^{-a_0 s} |w_j(t-s)| ds. \tag{3.7}
$$

Note convergence $w_j(\sigma) \to 0$ for $\sigma \to +\infty$ and all $j \in I_{n'} \subseteq I \cup \{1, \dots, n'-1\}$. For $j \in I$ this holds by assumption (3.3). For the complementary vertices $j \in \{1, \dots, n'-1\} \setminus I$ this holds by induction hypothesis. Since the integrals (3.7) converge by Lebesgue dominated convergence, for the uniformly bounded shifts of w_j, this implies

$$
\lim_{t \to +\infty} \int_0^t e^{-a_0 s} |w_j(t-s)| ds = 0. \tag{3.8}
$$

Since $\{1, \dots, n'-1\} \setminus I = \varnothing$ for $k = n' = 1$, this completes the induction for (3.4), and proves the lemma. $\square$

Lemma 3.2. *Let I be a feedback vertex set of the di-graph Γ of a dissipative nonautonomous regulatory ODE network (1.1). Assume continuity of the nonlinearities F_k, $\partial_z F_k$, bounded uniformly for $t \geq 0$ and bounded $|z|$, and assume the decay condition (1.5).*

Then I is a set of determining nodes of (1.1).

Proof.
Let $w(t) := \widetilde{z}(t) - z(t)$ for any two solutions $z(t)$, $\widetilde{z}(t)$ of the nonautonomous ODE network (1.1) such that $w_I(t) \to 0$ for $t \to +\infty$. We have to show $w(t) \to 0$ on all vertices.

We abbreviate (1.1) as $\dot{z} = F(t, z(t))$ and observe that the difference $w(t)$ satisfies the linear nonautonomous ODE

$$\dot{w}(t) = A(t)w(t) \tag{3.9}$$

where we define

$$A(t) := \int_0^1 \partial_z F(t, z(t) + \vartheta w(t)) d\vartheta. \tag{3.10}$$

Even though this definition of $A(t)$ clearly involves both nonlinear ODE solutions $z(t)$, $\widetilde{z}(t)$, we can safely use the fact that $w(t) := \widetilde{z}(t) - z(t)$ is a particular solution of the linear ODE (3.9). In fact we can rewrite (3.9) in the linear nonautonomous regulatory network form (3.1). Dissipativity of F implies uniform boundedness of $z(t)$, $\widetilde{z}(t)$, and of $z(t) + \vartheta w(t)$, for all $t \geq 0$. This implies uniform boundedness of $|b(t)|$. Decay condition (1.4) on F implies the uniform lower bound (3.2) required in lemma 3.1. Invoking lemma 3.1 for the particular solution $w(t) = \widetilde{z}(t) - z(t)$ completes the proof. □

4 Global attractors

In this section we prove the reconstruction theorem 1.6 on determinacy of global attractors $\mathcal{A}$ by the history time tracks $z_I(t)$ on the informative set I, alias the feedback vertex set, of the autonomous regulatory network (1.3). As in theorem 1.6, we assume dissipative C^1-nonlinearities F_k with decay condition (1.5) throughout the present section.

Proof of theorem 1.6.
Let $z(t)$, $\widetilde{z}(t)$ denote two solutions in the global attractor $\mathcal{A}$, for all nonpositive real times $t \in \mathbb{R}_-$. Note that z, $\widetilde{z}$ are globally bounded; see definition 1.4. We assume the C^2 history time tracks

$$\widetilde{z}_I(t) = z_I(t) \tag{4.1}$$

coincide, for all $t \in \mathbb{R}_-$, and we will show

$$\widetilde{z}(\tau) = z(\tau), \tag{4.2}$$

for all $\tau \in \mathbb{R}_-$. In particular this will show $\widetilde{z}(0) = z(0)$, proving injectivity of the informative projection $\mathcal{P}_I$ as claimed in (1.14).

Our proof of claim (4.2) proceeds along the lines of the proof of lemmas 3.1 and 3.2. We first define $w(t) := \widetilde{z}(t) - z(t)$. Because z, $\widetilde{z}$ are in the global attractor $\mathcal{A}$, they are uniformly bounded in C^2 – as is their difference w. We rewrite the resulting nonautonomous linear system (3.9), (3.10) for w as a nonautonomous linear regulatory network (3.1). The coefficients $a_k(t)$, $b_k^T(t)$ are uniformly bounded, because $F \in C^1$ and $z, \widetilde{z} \in \mathcal{A}$ are uniformly bounded. Similarly we obtain uniform decay $a_n(t) \geq a_0 > 0$ as required in (3.2).

We now proceed inductively, pretty much as in (3.6) – (3.8). The only modification will be that we shift the initial condition $w_{n'}(t_0)$ for the variations-of-constants formula of

$$\dot{w}_k(t) = -a_k(t)w_k(t) + b_k^T(t)w_{I_k}(t) \tag{4.3}$$

from $t_0 = 0$ to $t_0 = -\infty$. Specifically we have

$$\begin{aligned} w_k(t) =& \exp\left(-\int_{t_0}^{t} a_k(s)ds\right) w_k(t_0) + \\ &+ \int_{t_0}^{t} \exp\left(-\int_{s}^{t} a_k(\sigma)d\sigma\right) b_k^T(s)w_{I_k}(s)ds \end{aligned} \tag{4.4}$$

with $a_k(s) \geq a_0 > 0$ and uniformly bounded $b_k(s)$, $w_k(s)$. Therefore we may pass to the limit $t_0 \to -\infty$ in (4.4), for any fixed $t \in \mathbb{R}_-$. Since the first exponential in (4.4) converges to zero we obtain the convergent integral representation

$$w_k(t) = \int_{-\infty}^{t} \exp\left(-\int_{s}^{t} a_k(\sigma)d\sigma\right) b_k(s)w_{I_k}(s)ds. \tag{4.5}$$

By labeling order (2.1), this becomes a recursion for $n' = k = 1, \ldots, N'$ outside the feedback vertex set I. By assumption we have

$$w_I(t) = \widetilde{z}_I(t) - z_I(t) \equiv 0 \tag{4.6}$$

on I itself. Therefore, induction over $n' = k$ proves $\widetilde{z}(t) - z(t) = w(t) = 0$ for all $t \in \mathbb{R}_-$. This proves theorem 1.6. $\square$

As a corollary to theorem 1.6 we recover the result of [MoSa10] on stationary solutions of autonomous regulatory networks (1.1), (1.10).

Corollary 4.1. [MoSa10] *Let I be an informative set of the di-graph Γ of a dissipative autonomous regulatory ODE network (1.3) with decay condition (1.4). Let z and $\widetilde{z}$ be stationary solutions, i.e. $F(z) = F(\widetilde{z}) = 0$, which coincide on the informative set, i.e. $\widetilde{z}_I = z_I$.*

Then z and $\widetilde{z}$ are identical, $\widetilde{z} = z$.

Proof.
By corollary 2.4 the informative set I is a feedback vertex set. By definition 1.4 stationary solutions z, $\widetilde{z}$ belong to the global attractor $\mathcal{A}$. By theorem 1.6 the assumption $\widetilde{z}_I = z_I$ an the feedback vertex set I implies $\widetilde{z} = z$ are identical, as claimed. $\square$

5 Mathematical examples

So far, we have proved theorem 1.6 on the reconstruction of global attractors, and the if-part of theorem 1.3 on the determing property of feedback vertex sets. We now illustrate these results by five mathematical examples of specific autonomous regulatory networks

$$\dot{z}_k = F_k(z_k, z_{I_k})\,. \tag{5.1}$$

Unless stated otherwise, nonlinearities are C^1, dissipative, and satisfy the decay condition (1.4), i.e.

$$\partial_1 F_k(z_k, z_{I_n}) < 0 \tag{5.2}$$

for all k, uniformly for bounded $|z|$. We begin with acyclic di-graphs Γ, in example 5.1. Examples 5.2 and 5.3 examine the case of a single self-loop Γ and a loop Γ of length two, respectively. As a three-dimensional example we discuss feedback vertices I of the celebrated Lorenz equations in example 5.4. Example 5.5 returns to the linear autonomous version of the Frobenius graph of Figure 1.1 which features a one-point feedback vertex set I. All examples except 5.4 will also be used in the proof of the only-if-part of theorem 1.3.

5.1 Example: acyclic regulatory networks

Acyclic regulatory networks (5.1) allow for an empty feedback vertex set, $I = \varnothing$, by definition. The if-part of feedback vertex theorem 1.3, as proved in section 3, then asserts that the empty set I is determining for the dynamics of (5.1). In view of definition 1.1 this means that

$$\widetilde{z}(t) - z(t) \underset{t\to+\infty}{\longrightarrow} 0\,, \tag{5.3}$$

for any two solution z, $\widetilde{z}$. By degree theory the global attractor $\mathcal{A}$ of (5.1) contains a stationary solution $z(t) \equiv z$, see for example [Ha88]. By (5.3), this stationary solution is unique and globally attracting. In particular the global attractor $\mathcal{A}$ is just that globally asymptotically stable stationary point, $\mathcal{A} = \{z\}$. This is also the appropriate interpretation of the attractor reconstruction theorem 1.6 for $I = \varnothing$.

5.2 Example: the single self-loop

Autonomous regulatory networks (5.1) for which the di-graph Γ consists of a single self-loop Γ can be written as a single scalar ODE

$$\dot{z}_1 = F(z_1)\,, \tag{5.4}$$

$z_1 \in \mathbb{R}$. The decay condition (1.5) is void, due to the self-loop. Dissipativity is equivalent to

$$F(z)z < 0 \tag{5.5}$$

for $|z| \geq C$ large enough. Obviously $I = \{1\}$ is the only feedback vertex set. See Figure 3(a). The global attractor $\mathcal{A}$ is the closed interval with endpoints given by the minimal and maximal zero of F. Explicit examples are provided by polynomials

$$F(z) = -z^{2n+1} + \ldots + c_0 \tag{5.6}$$

of odd degree. In particular any number of coexisting equilibia may arise in non-monotone regulatory networks with a single feedback vertex.

The assertion of the if-part of feedback vertex theorem 1.3 becomes void because the only possible feedback vertex set $I = \{1\}$ already consists of all

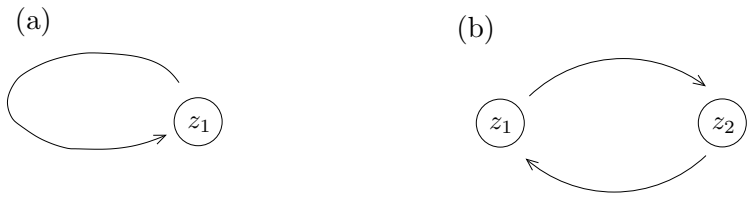

Figure 3: Di-graphs Γ of a single self-loop (a), and a single cycle of length 2, (b).

vertices of Γ. The assertion of the attractor reconstruction theorem 1.6 is likewise trivial because the correspondence between initial conditions $z_1(0)$ and history time tracks $z_1(t)$ is unique.

Note however how the above example proves the converse only-if-part of feedback vertex theorem 1.3 for the single self-loop γ. Indeed $I = \varnothing$, the only other option for a set of determining nodes, fails by example 5.1 whenever the nonlinearity $F(z)$ possesses more than a single real zero.

5.3 Example: single loops of length two

For single loop di-graphs Γ of two vertices, the autonomous regulatory network (5.1) reads

$$\begin{aligned} \dot{z}_1 &= G_1(z_1, z_2) \\ \dot{z}_2 &= G_2(z_1, z_2) \end{aligned} \tag{5.7}$$

with decay condition (1.5) in the form

$$\partial_1 G_1 < 0, \quad \partial_2 G_2 < 0\,. \tag{5.8}$$

Obviously $I = \{1\}$ or $I = \{2\}$ can equally serve as a non-unique minimal feedback vertex set. See Figure 3(b). For genericity we assume equilibria of (5.7) to be hyperbolic.

The dynamics of (5.7) is gradient-like. Indeed decay condition (5.8) asserts negative divergence of (5.7) and hence precludes periodic and homoclinic orbits as well as any heteroclinic loops. Theorem 1.6 and the if-part of theorem 1.3 assert how monitoring the history time track of any single component of

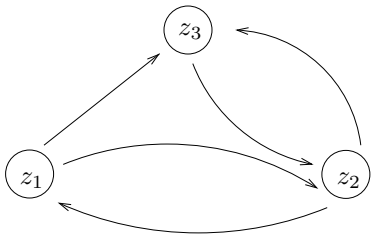

Figure 4: The di-graph Γ of the Lorenz system (5.10), viewed as a regulatory network.

$z = (z_1, z_2)$ is sufficient to determine trajectories in the global attractor $\mathcal{A}$, or the asymptotic dynamics of any trajectory.

To address the only-if-part of feedback vertex theorem 1.3 we observe that, again, the only other option $I = \varnothing$ fails to be determining. Indeed example 5.1 would then require stationary solutions to be unique. An easy dissipative example (5.7) with multiple stationary solutions, however, is given explicitly by

$$\begin{aligned} \dot{z}_1 &= a z_2 - z_1 \\ \dot{z}_2 &= \sin z_1 - z_2 \end{aligned} \tag{5.9}$$

with $a > 1$.

5.4 Example: the Lorenz attractor

The celebrated Lorenz equations are

$$\begin{array}{rcccc} \dot{z}_1 &=& \sigma z_2 & - & \sigma z_1 \\ \dot{z}_2 &=& \rho z_1 - z_1 z_3 & - & z_2 \\ \dot{z}_3 &=& z_1 z_2 & - & \beta z_3 \end{array} \tag{5.10}$$

with positive parameters σ, ρ, β; [Lo63]. See Figure 4 for the associated di-graph Γ which casts the Lorenz system into the form of an autonomous regulatory network. Clearly $I = \{2\}$ is a minimal feedback vertex set of Γ.

The literature on the dynamics of the Lorenz system abounds. See [Sp82] for an early survey. Dissipativeness of the Lorenz system is known. Chaoticity

has been proved for suitable parameters; see [Mi&al01, Tu02] and the earlier references there. In addition a plethora of bifurcations attest to multiple stationary solutions, homoclinicity, period doubling cascades, and so on.

Again attractor reconstruction theorem 1.6 asserts that all the fairly complicated dynamics of the whole Lorenz system can be faithfully represented by only monitoring the history time track $z_2(t)$, $t \in \mathbb{R}_-$. The if-part of feedback vertex theorem 1.3 makes a similar assertion for the large time asymptotics of any Lorenz trajectory $z(t)$, $t \geq 0$, not necessarily restricted to the Lorenz attractor itself.

Our approach applies, as well, to many other chaotic systems of related structure. For example we mention the chaotic Chen system of which global boundedness has recently been proved in [BaCh11].

5.5 Example: Frobenius matrices

We consider the Frobenius di-graph Γ of Figure 1 with autonomous linear $F_k(z_k, z_{I_k})$. More specifically we consider the system

$$\begin{array}{rcccl} \dot{z}_1 & = & z_2 & - & a_0 z_1 \\ \dot{z}_2 & = & z_3 & - & a_0 z_2 \\ & \vdots & \vdots & \vdots & \\ \dot{z}_{N-1} & = & z_N & - & a_0 z_{N-1} \\ \dot{z}_N & = & -c_0 z_1 - \ldots - c_{N-1} z_N & - & a_0 z_N \end{array} \tag{5.11}$$

In the linear setting (3.1) this corresponds to the choices $a_k(t) = -1 < 0$, $I_k = \{k+1\}$, $b_k(t) = +1$, except for $I_N = \{1, \ldots, N\}$ and $b_{Nj} = -c_{j-1}$. In short,

$$\dot{z} = Cz - z \tag{5.12}$$

if we choose $a_0 = 1$. Here C is a Frobenus matrix with characteristic polynomial

$$p_C(\lambda) = \lambda^N + c_{N-1}\lambda^{N-1} + \ldots + c_0\,. \tag{5.13}$$

This is obvious because $\dot{z} = Cz$ is equivalent to the N-th order scalar equation $z_1^{(N)} + \ldots + c_0 z_1 = 0$. As we have already observed in section 1 the minimal

feedback vertex set I of Γ is $I = \{N\}$.

The spectrum $\Lambda := \{\lambda_1, \ldots, \lambda_N\}$ of $C - \mathrm{id}$ in (5.12) can be chosen arbitrarily via the shifted zero set (5.14) of the characteristic polynomial $p_C(\lambda + 1) = 0$ and the resulting coefficients $c_0, \ldots, c_{N-1}$. Decay condition (1.5) holds by construction. If desired, dissipativity can be enforced, e.g., by a nonlinear modification

$$a_0 = a_0(z) = 1 + \chi(z^2) \tag{5.14}$$

where the smooth real function χ is zero, say for $z^2 \leq 1$, and z^2 for large arguments z^2.

We now interpret the results of the if-part of feedback vertex theorem 1.3 and of reconstruction theorem 1.6 for the purely linear system (5.12). For simplicity we only consider simple eigenvalues λ_j and avoid growing solutions by the assumption $\mathrm{Re}\ \Lambda \leq 0$. Decaying eigenvalues $\mathrm{Re}\ \lambda_j < 0$ neither contribute to the solution differences of theorem 1.3, asymptotically, nor to the linear analogue of the global attractor $\mathcal{A}$, namely the set of solutions $z(t)$ which are bounded for all positive and negative real times t. Therefore, we only discuss the purely imaginary part $\mathrm{Re}\ \lambda_k = 0$ of the spectrum Λ.

Suppose $\lambda_k = 0$ is a simple eigenvalue of $C - \mathrm{id}$. The associated eigenvector $z \neq 0$, which defines a line of stationary solutions of (5.12), possesses a component $z_N \neq 0$ at the determining feedback vertex set $I = \{N\}$. The component z_N therefore allows us to monitor the stationary solutions.

Similarly the eigenvector $z^j \neq 0$ of any nonzero purely imaginary eigenvalue $\lambda_j = i\omega_j$ possesses nonzero feedback vertex component z^j_N. Indeed

$$i\omega_j z^j_k = \dot{z}_k = z^j_{k+1} - z^j_k\,, \tag{5.15}$$

for $k = 1, \ldots, N-1$ would likewise force all components z^j_k to vanish, in case $z^j_N = 0$. This allows us to detect a single pair of simple eigenvalues $\pm i\omega_j$ on the imaginary axis, via the determining history time track $z_N(t)$.

More importantly, theorems 1.3 and 1.6 assert, for any simple pure imaginary spectrum, that the time track $z_N(t)$ also allows us to track the full dynamics of (5.12). Tracking works at least asymptotically for $t \to +\infty$, in presence of other decaying eigenvalues $\mathrm{Re}\ \lambda_k < 0$. In absence of decaying components we are on the linear analogue of the global attractor $\mathcal{A}$ and can faithfully

reconstruct the full dynamics $z(t)$ from only the history time track $z_N(t),\ t \leq 0$.

For example let all eigenvalues be simple purely imaginary pairs $\pm i\omega_j$ with distinct $\omega_j > 0$. Then any solution $z(t)$ of (5.12) is quasiperiodic and can be written as

$$z(t) = \sum_j \alpha_j e^{i\omega_j t} z^j \,, \tag{5.16}$$

in abbreviating complex notation. In particular

$$z_N(t) = \sum_j \alpha_j e^{i\omega_j t} z_N^j \tag{5.17}$$

with $z_N^j \neq 0$ for all j. Via the Fourier averages

$$\begin{aligned} (Mz_N)(\omega) &:= \lim_{T\to-\infty} \frac{1}{T} \int_0^T z_N(t) e^{-i\omega t} dt = \\ &= \begin{cases} \alpha_j z_N^j & \text{for} \quad \omega = \omega_j \,, \\ 0 & \text{otherwise} \end{cases} \end{aligned} \tag{5.18}$$

of the determining feedback vertex history time track $z_N(t)$ we can recover the complete set of time periodic spectral components $\pm i\omega_j$ which contribute to the full quasiperiodic solution $z(t)$ via $\alpha_j \neq 0$. This follows from reconstruction theorem 1.6 or, quite explicitly in this easy linear case, because $z_N^j \neq 0$ for all j.

6 From determining nodes to feedback vertices

In this section we prove the only-if-part of feedback vertex theorem 1.3 on determining nodes of nonautonomous regulatory networks, as formulated in lemma 6.1 below. Our proof proceeds by the contrapositive: assuming $I \subseteq \{1, \ldots, N\}$ is not a feedback vertex set of the di-graph γ, we construct nonlinearities F_k such that I is not a set of determining nodes. Our constructions of F_k will be based on the examples discussed in section 5. All

constructions will feature multiple stationary or periodic solutions $z(t)$ of autonomous regulatory networks (1.3) which become indistinguishable when restricted to I. Where we refer to the linear Frobenius example 5.5, the dissipative modification (5.14) will tacitly be assumed.

Lemma 6.1. *Consider autonomous regulatory* ODE *networks (1.3) with associated di-graph* Γ. *Assume* $I \subseteq \{1, \dots, N\}$ *is not a feedback vertex set of* Γ.

Then there exist smooth dissipative nonlinearities F_k *with decay property (1.5) such that* I *is not a set of determining nodes for the dynamics of (1.3).*

Proof.
Because I is not a feedback vertex set, definition 1.2 implies that the remaining graph $\Gamma \setminus I$ possesses a cycle, say $1 \to m \to m-1 \to \dots \to 1$. Outside the cycle vertices $M = \{1, \dots, m\}$ we simply choose uniform decay

$$F_k(z_k, z_{I_k}) := -z_k \,. \tag{6.1}$$

In particular this ensures global asymptotic stability $z_k(t) \to 0$ for all $k \notin M$, and hence for all $k \in I \subseteq \Gamma \setminus M$. The dynamics on M is therefore invisible on I. On the cycle M itself we choose

$$F_k(z_k, z_{I_k}) = F_k(z_k, z_{k+1}) \tag{6.2}$$

for indices in M mod m. In particular $I_k = \{k+1\}$ mod m.

Our construction of F_k now reduces to the case where the remaining graph $\widetilde{\Gamma} := \Gamma \setminus I$ is a single cycle with vertices M. The dynamics on M is invisible to I. Hence it is sufficient to construct smooth dissipative nonlinearities F_k on M with decay property (1.5) such that multiple stationary or periodic solutions arise. We treat the cases $m = 1, 2$, and $m \geq 3$ separately.

For $m = 1$ the cycle graph on $M = \{1\}$ is a single self-loop as discussed in example 5.2. Since multiple stationary solutions can arise in that example, the set I is not a set of determining nodes.

Analogously, example 5.3 of a single loop with two vertices settles the case $m = 2$.

The linear Frobenius example 5.5 suggests an alternative way, albeit less generic, to settle the case of arbitrary cycles $M = \{1, \dots, m\}$. Ignoring

dissipativity, which was already settled in (5.14), we choose

$$F_k(z_k, z_{k+1}) := z_{k+1} - z_k \tag{6.3}$$

for any fixed $m \geq 1$ and indices mod m. By (5.13), (5.14) the resulting characteristic polynomial for the eigenvalues λ of $\dot{z} = Cz - z$ on $M = \{1, \ldots, m\}, z$ is

$$(\lambda + 1)^m - 1 = 0\,. \tag{6.4}$$

As a spectrum we obtain the shifted roots of unity

$$\lambda = e^{2\pi i k/m} - 1\,, \tag{6.5}$$

$k = 0, 1, \ldots, m-1$, with $\mathrm{Re}\,\lambda < 0$ except for a trivial simple eigenvalue $\lambda = 0$. The associated trivial eigenspace of $k = 0$ spanned by $(1, \ldots, 1)$ provides multiplicity of stationary solutions, as claimed. Similarly, a modification of the last equation $\dot{z}_m = -c_0 z_1 - z_m$ with suitable $c_0 < 0$ can provide multiplicity of periodic solutions, due to purely imaginary eigenvalues.

This proves the lemma and completes the proof of theorem 1.3. □

On the cycle M itself the above linear construction can be perturbed slightly to generic and robust situations, if desired. This will produce multiple stable and unstable hyperbolic stationary or periodic solutions.

One may object that Γ is not the minimal graph compatible with the above construction of a feedback cycle M disjoint from I. But, strictly speaking, minimality of Γ has not been required. Speaking less strictly, though, a slightly more intricate construction than we present here can also accommodate the additional requirement of minimality. We only have to ensure that the coupling via the graph Γ remains constant on the particular values of the multiple stationary or periodic solutions constructed on the cycle M. In view of the ubiquitous switching behavior of nonlinearities which model biological regulatory networks, such local constancy may well occur. See also the ascidian network example of section 7.1 as discussed in section 4-2 of [Mo&al13].

7 Applications to biological networks

Modern biology provides many examples of large networks which describe regulations between a large number of species of molecules, such as genes,

proteins or ions. It is widely believed that the dynamics of molecular activities based on such regulatory networks are the origin of biological functions. However, a variety of obstacles still impede attempts to systematically study the dynamics of biological systems based on the knowledge of regulatory networks. The regulatory networks in many studies of biological systems are possibly still incomplete, at present, because of the difficulty and working costs of experimental procedures to identify regulatory edges. In addition, information on the regulatory network alone may not be sufficient to determine the resulting dynamics. The regulatory edges only provide information on dependencies between activities of bio-molecules in the system. They fail to provide necessary quantitative details like the regulatory functions, the parameter values of reaction rates, and initial conditions.

In the present section we therefore identify key vertices of biological regulatory networks, called informative nodes in [MoSa10], which faithfully trace the full dynamics of the network; see our feedback vertex theorem 1.3 and our attractor reconstruction theorem 1.6. The specific dynamics, to be experimentally traced on the feedback vertex set, will of course depend on further quantitative details like regulatory functions, reaction rates, and initial conditions. For identification purposes via determining nodes, or for reconstruction of the dynamics on the global attractor, such quantitative details are irrelevant. Incompleteness of the theoretical regulatory network, however, may show up by inconsistencies of the traced dynamics.

We provide three biological applications of our theory in this section. We discuss prominent regulatory networks from the biology literature for cell-differentiation, signal transduction, and circadian rhythms. In the first two examples, we determine very small informative sets from rather large regulatory networks. We also discuss the possible inability of these networks to generate observed biological phenomena. This directly implies that unknown edges or unknown molecules may exist which are responsible for these observed phenomena. In the last example, we numerically demonstrate how to control a system by a minimal and sufficient number of key variables given by an informative set. For a more detailed analysis from a biological view point we refer to the companion paper [Mo&al13].

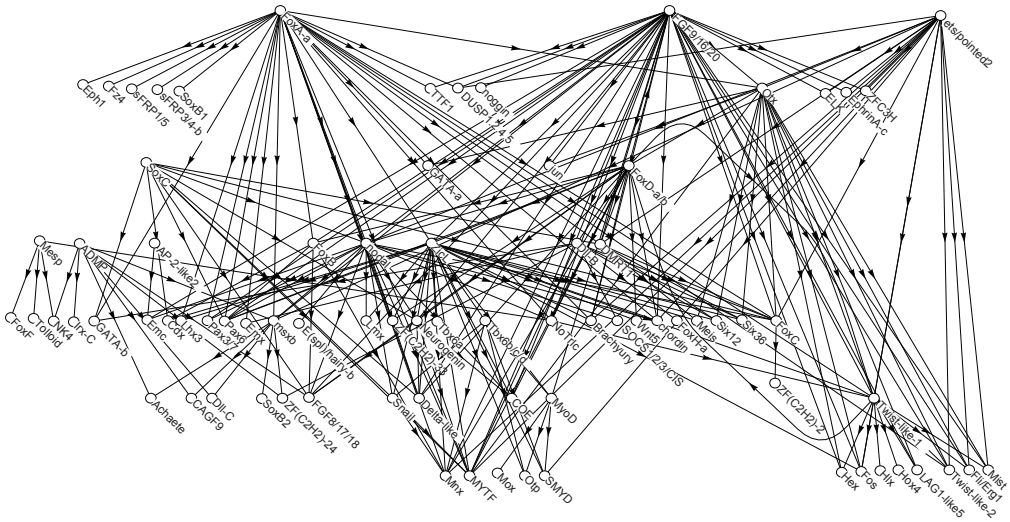

Figure 5: A gene regulatory network for cell-differentiation in early development of the ascidian *Ciona intestinalis*, redrawn based on [Im&al06]. Our redrawing removed 16 edges of self-repression from the original network because self-repression can be subsumed under decay condition (1.5).

7.1 Ascidian network

We consider a gene regulatory network determined by [Im&al06], which is responsible for cell-differentiation in the development of the ascidian *Ciona intestinalis* from the 16-cell stage to the tail-bud stage. In the focal period, the difference in gene activities between cells progresses with time, and 13 different gene expression patterns are observed at the final, tail-bud stage, depending on the position of cells in the body. The system is expected to be flexible enough to produce many steady states of gene activities, which correspond to differentiated cells. In the study 80 genes were identified to control embryogenesis of *Ciona*. The regulatory interactions between these genes were determined by perturbation analysis, where the activity of one gene was manipulated and the effects were examined.

The network determined by [Im&al06] possesses 80 vertices and regulatory edges between them. The regulatory edges are categorized into two classes, activation and repression. As we have discussed in connection with our decay condition (1.5) we do not distinguish between activation and repression here,

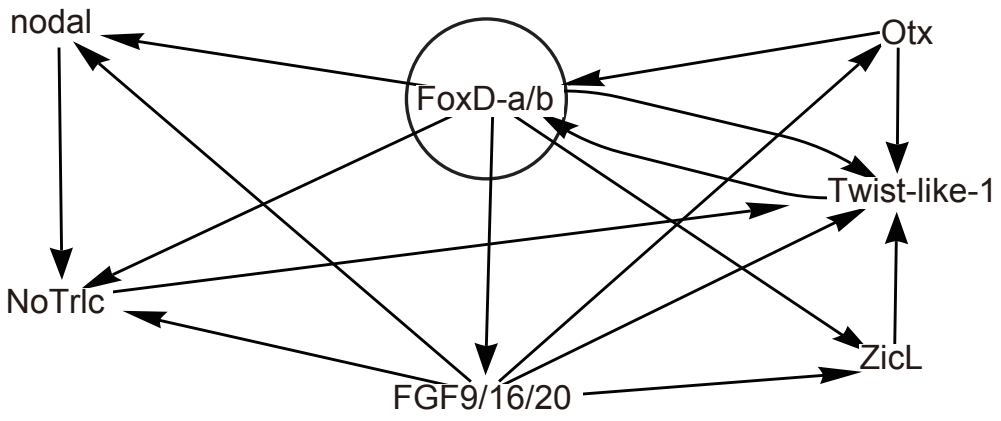

Figure 6: A gene regulatory network for cell-differentiation of the ascidian *Ciona intestinalis* after removing vertices without input or output from the network in Figure 5. The network possesses a single feedback vertex FoxD-a/b.

except for self-regulatory edges. There are 16 genes with self-regulatory edges, all of which are self-repressions. We remove these self-repressive edges from the network because any self-repression can be subsumed under the decay condition (1.5), i.e. a negative partial derivative of F_k with respect to the argument z_k. See Figure 5 for the resulting regulatory network.

As a preparation we removed the vertices which do not regulate any vertices or which do not receive any regulations. These top or bottom genes converge to fixed inputs or provide outputs of the system which do not contribute to the diversity of attractors. The removal procedure was repeated while the network had vertices with no input or no output. Note that this iterative reduction preserves all di-cycles, and hence preserves any minimal feedback vertex set. We obtained the reduced network of Figure 6 with only 7 vertices. The network clearly possesses a unique minimal feedback vertex set which consists of only a single feedback vertex, FoxD-a/b.

All long-term dynamics on the global attractor possibly generated by this gene regulatory network can therefore be identified by measurement of the activity of the single gene FoxD-a/b. If the 13 different gene expressions observed in differentiated cells at the tail-bud stage are stable equilibria of

this system, their diversity should be identified by the activity of FoxD-a/b. Actually[Im&al06] provided data of gene expressions in differentiated cells. However, they are interpreted in a discrete and binary manner, i.e. active (1) or inactive (0), as usual in many studies of present experimental biology. Of course, the diversity of 13 different stationary gene expression patterns cannot be identified in a single binary space which consists of only two points.

There are multiple ways to resolve this problem. First, we may be able to identify 13 different gene expression patterns if we measure the activity of the FoxD-a/b gene quantitatively. The second possibility is that gene expressions at the tail-bud stage may not be stable equilibria of the ordinary differential equation system (1.3) associated to the regulatory network. A third possibility is that the regulatory network in [Im&al06] may not be complete and there are unknown regulatory edges that would produce feedback loops which are not cut by FoxD-a/b.

7.2 Signal transduction network

A variety of cell responses are induced by the surrounding environment or by other signals from outside a cell. The signaling pathway downstream of the epidermal growth factor (EGF) receptor has been studied in mammalian cells. It has been shown to regulate a large diversity of cell responses including proliferation, migration, oncogenesis, and apoptosis. The process by which the growth factor signals induce cell reactions can be described roughly as follows: by the ligand-binding to the EGF receptor, the tyrosine-kinase activity of the receptor is induced. The activated EGF receptors phosphorylate and activate the target proteins. The activation of proteins causes activation of other species of molecules and the activation signal is transferred through a series of species of molecules, sequentially. The signal is finally transferred into the nucleus, regulates gene expressions and causes changes in macroscopic cell behavior. The diverse reactions of the cell are produced by this signal transduction system. In other words, the signal transduction network is a system for the determination of the macroscopic behavior of mammalian cells after receiving the signal molecule stimulus from outside. Many studies of signal transduction focus on the crucial question how a single system produces multiple output responses depending on the stimulus inputs from

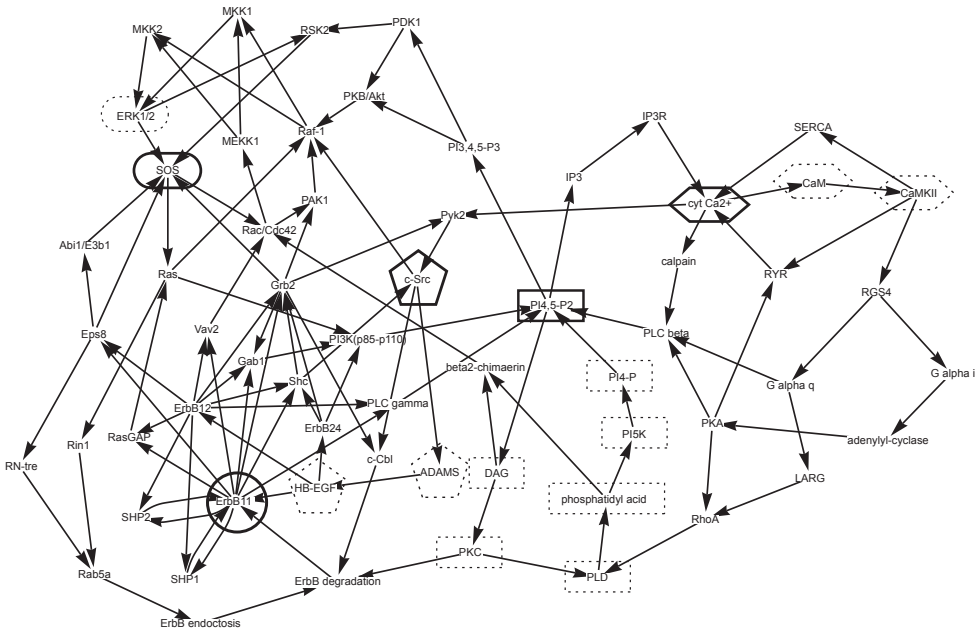

Figure 7: Signal transduction network downstream of the EGF receptor, redrawn based on [Oda05]. The vertices without input or output are removed from the original. We mark one particular choice of a minimal feedback vertex set with five elements by circles and polygons with solid line boundaries. Corresponding elements to construct alternative minimal feedback vertex sets are shown by corresponding polygons with broken line boundaries. See also table 1.

outside the cells.

We analyze a regulatory network of signal transduction suggested by [Oda05]. The authors collected information on pathways of signal transduction from published papers, which are determined by various experimental methods. They summarized the information of regulation between molecules, and constructed a complex regulatory network of 113 species of molecules including kinases, phosphatase, or ions like Ca^{2+}, and many regulatory edges between them. There is no self-regulatory edge in this network. As a preprocessing we removed vertices without input or output as described in our above analysis for the ascidian network, see section 7.1. The resulting reduced network is still complex and possesses 61 vertices.

We adopt a method of computer-aided search to determine a feedback vertex set of minimal size. Our search algorithm is simple, using only definition 1.2 of a feedback vertex set, and exhaustive, starting from smaller to larger size of candidate sets. We found 36 ways to select the feedback vertex set with a minimum of five vertices.

(1)	(2)	(3)	(4)	(5)	# combinations
ErbB11	SOS ERK1/2	HB-EGF c-Src ADAMS	cyt Ca^{2+} CaM CaMKII	PI4,5-P2	2*3*3=18
ErbB11	SOS	HB-EGF c-Src ADAMS	cyt Ca^{2+}	PI4-P DAG PKC PLD phosphatidyl acid PI5K	3*6=18

Table 1: List of 36 different choices of feedback vertex sets of the signal transduction network. The last column lists the number of different choices which arise combinatorially, in each row.

Table 1 shows the possible choices of vertices to form a minimal feedback vertex set. The vertices in these sets are categorized into five groups, which are shown in different shapes of polygons in Figure 7.

The regulatory network of signal transduction is expected to model a broad variety of dynamic responses in the global attractor, depending on the stimulus signals from outside the cell. Actually this interpretation is still hypothetical and is not yet confirmed by experiments. We need time-series data of activities of key molecules to faithfully represent the dynamics of the system. For this purpose we have to select which molecules to track, because it is still difficult to simultaneously measure the activities of many molecules with sufficient time-resolution for discussing their dynamics. Our theory provides rational criteria to select those key molecules. Measuring the time tracks of five feedback vertices experimentally in different environments, after receiving the stimulus signals, will faithfully represent the diversity of the dynamical response of the whole system. If we discover, on the other

hand, that the time tracks of five feedback vertices are not sufficient to explain all of the expected reactions, then we may be forced to conclude that the original network missed some important edges or molecules.

7.3 Control of mammalian circadian rhythm

In this example, we explore a control aspect of our theory. We demonstrate that the dynamics of the whole system can be controlled by controlling the dynamics of only a feedback vertex set. Note that our setting does not involve control via any feedback loop. Rather we clamp the feedback vertices to follow a known, desirable solution of the original full system for all forward times. This forces the full system to follow that precise same trajectory, eventually, independently of any other initial conditions outside the feedback vertex set. For further comments on our open-loop approach see sections 7.4 and 8.4.

Mammalian circadian rhythms in mice have been studied well, experimentally. Four major genes are involved in the system: *Per1*, *Per2*, *Cry1* and *Cry2*. The regulations between genes and the interactions between these proteins have been examined in detail. The system in a normal animal exhibits periodically oscillating gene activities. Many mathematical models for the system were proposed and studied. At present, all mathematical models include assumptions on experimentally unverified facts, in particular in the specific formulae and parameters of the regulatory functions. In some studies models were analyzed mathematically or numerically and conditions for periodic oscillations were determined.

For our numerical experiments we use a mathematical model proposed by [Mi09], which includes 21 variables and 132 parameters. The ordinary differential equations and our choice of parameter values are detailed in the Appendix. The regulatory network is shown in Figure 8a. The size of the feedback vertex set I is 7, $I = \{$PER1, PER2, CRY1, CRY2, RORc, CLK/BMAL1, CLK$\}$. We found that the dynamics of the model shows multiple asymptotic behaviors including two stable periodic oscillations (P1 and P2), one unstable periodic oscillation (UP), and one unstable stationary point (USS) under a choice of parameter values, which are different from the original values in [Mi09]. Figure 8c shows the dynamical trajectory of these asymptotic behaviors on two dimensional space, *Per1* mRNA and *Per2*

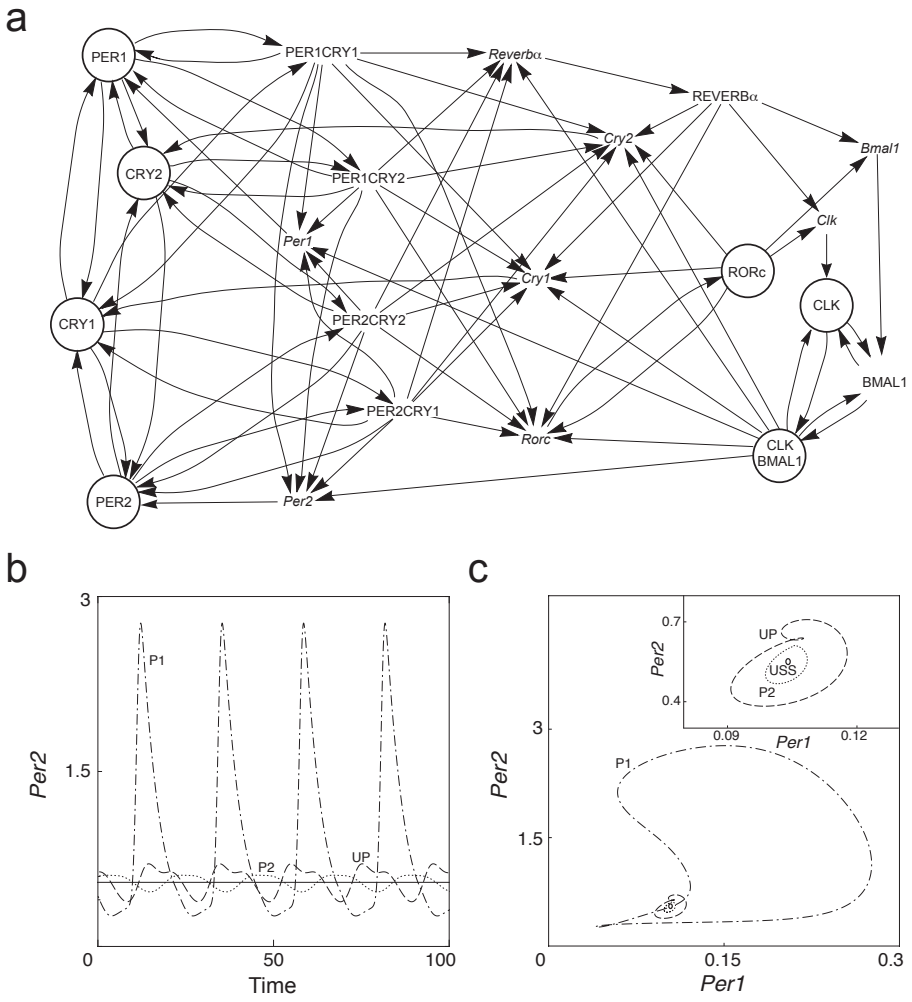

Figure 8: Dynamical system of mammalian circadian rhythms. (a) A regulatory network with 21 variables, redrawn after [Mi09]. Our choice of a feedback vertex set I is marked by circles. (b) Trajectories of two attractors, period1 (P1) and period2 (P2), unstable period (UP) and unstable stationary state (USS), represented by time tracks of the variable *Per2*. Vertical axis: *Per2*, horizontal axis: time t. Dotted and broken curve: P1, dotted curve: P2, broken curve: UP, solid line: USS. (c) Two stable periods and an unstable period, and an unstable stationary state, identified by the two variables *Per1* and *Per2*. These two variables are not in the feedback vertex set. Broken or dotted curves identify the same cycles as (b).

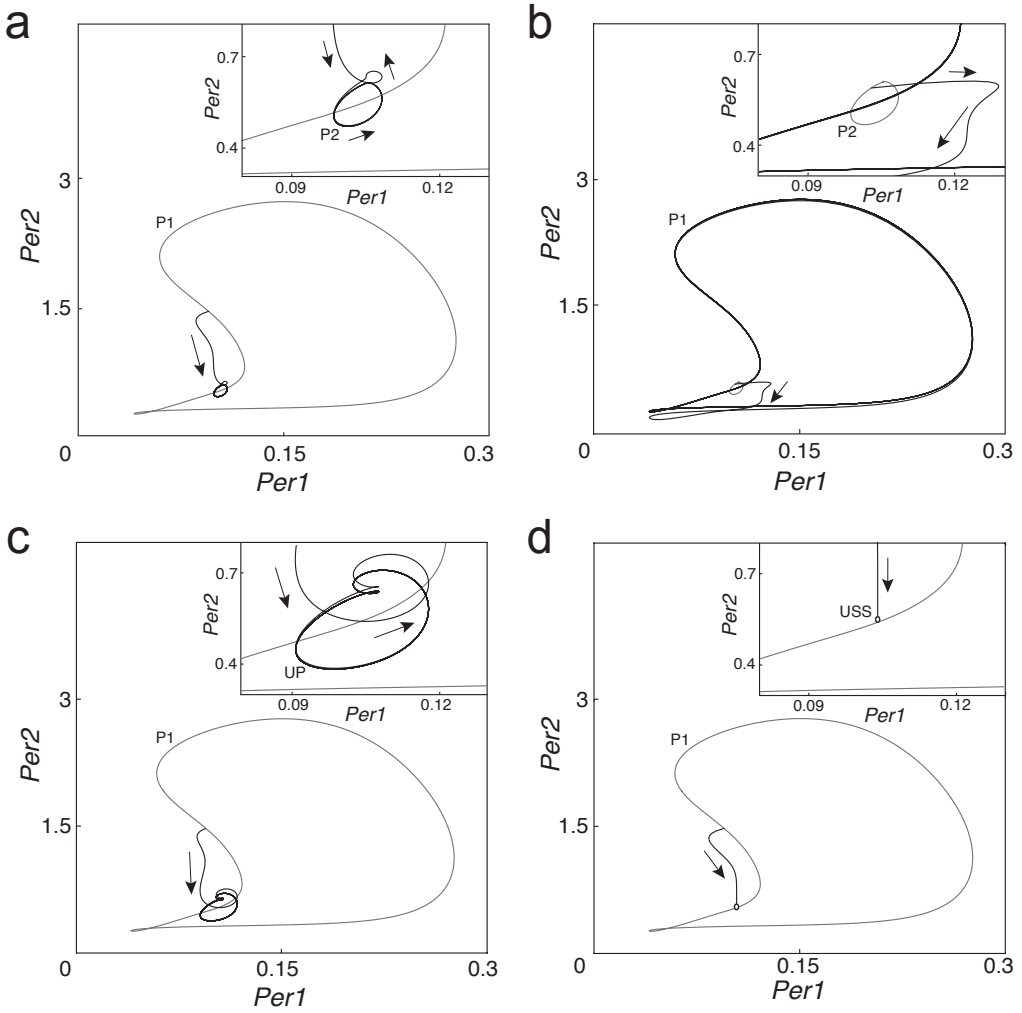

Figure 9: Numerical trajectories of successful open loop controls of circadian rhythms by the full feedback vertex set I. The horizontal and vertical axes are *Per1* and *Per2*, respectively, which are not in the chosen feedback vertex set I. Zooms into P2, UP, and USS are shown as top-right inserts. (a) Trajectory of the control experiment "from P1 to P2" is shown by black solid curve. Known stable cycles P1 and P2 are shown by gray solid curves. (b) Black solid: trajectory of the control experiment "from P2 to P1". Gray solid: P1 and P2. (c) Black solid: trajectory of the control experiment "from P1 to UP". Gray solid: P1 and UP. (d) Black solid: trajectory of the control experiment "from P1 to USS". Gray solid: P1, open dot: USS.

mRNA.

We performed four numerical experiments, controlling "from P1 to P2", "from P2 to P1", "from P1 to UP" and "from P1 to USS". We examined whether the system is controlled by prescribing the time tracks of the 7 informative variables in the feedback vertex set I. As a preparation we calculated the time tracks of each informative variable z_k on the four invariant sets, P1, P2, UP and USS, by numerical simulation, i.e. $z_k^{\mathrm{P1}}(t)$, $z_k^{\mathrm{P2}}(t)$, $z_k^{\mathrm{UP}}(t)$ and $z_k^{\mathrm{USS}}(t)$ $(0 \leq t \leq T)$.

The protocol of our numerical experiment called "from P1 to P2" is the following: the forward time tracks of the 7 informative variables are prescribed to follow their values $z_I^{\mathrm{P2}}(t)$, as on P2. The dynamics of the remaining 14 variables are calculated by the remaining ODEs of the system, and the initial state of these remaining variables is chosen to coincide with a point on the P1 trajectory. We used different points on the P1 orbit as initial state.

The results did not depend on the initial point on P1, as much as we examined. We observed how the dynamical trajectory starting from the P1 soon left that stable periodic orbit, and quickly converged to the competing P2 orbit. The total system finally shows periodic oscillation on the P2 orbit.

Following the analogous protocol, we examined the opposite experiment "from P2 to P1". The tracks of the 7 informative variables in the feedback vertex set I are now prescribed to follow their values $z_I^{\mathrm{P1}}(t)$ on P1, and the dynamics of the remaining 14 variables are calculated by the remaining ODEs with an initial state on P2. In the experiment we observed that the total system soon left P2, this time, and converged to P1 following the prescribed informative dynamics $z_I^{\mathrm{P1}}(t)$.

Next we examined the experiment "from P1 to UP", where the tracks of the 7 informative variables in the feedback vertex set I are prescribed to follow their values $z_I^{\mathrm{UP}}(t)$ on UP, and the dynamics of the remaining 14 variables are calculated by the remaining ODEs with an initial state on P1. It is interesting how control of the feedback vertex set, only, forced the total system to stably converge towards the periodic oscillation UP, even though this oscillation was unstable in the full system.

Finally we examined the numerical experiment "from P2 to USS": the 7 informative variables $z_I(t)$ in the feedback vertex set are fixed at their constant

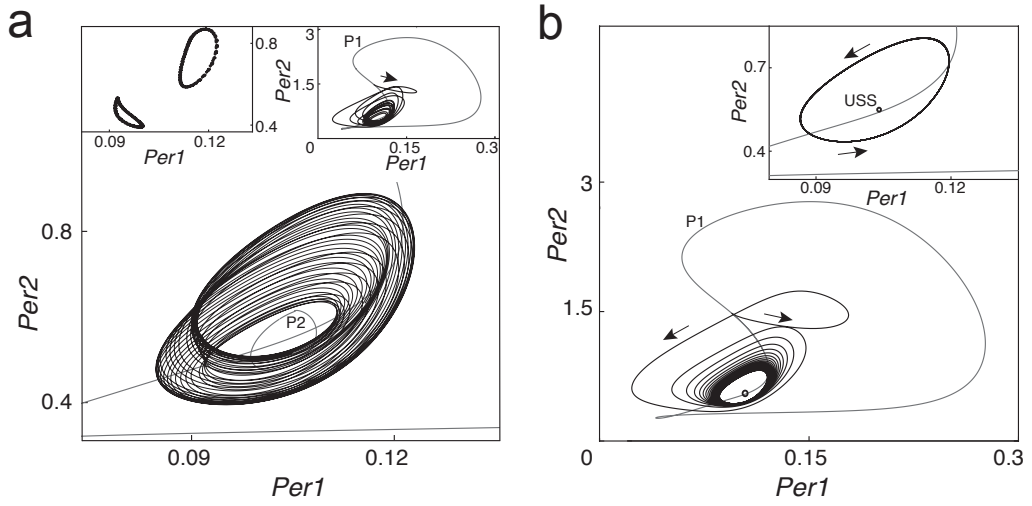

Figure 10: Numerical trajectories of failed open loop controls of circadian rhythms by the reduced vertex set $I' = I \setminus \{\text{CLK, CLK/BMAL1}\} = \{\text{PER1, PER2, CRY1, CRY2, RORc}\}$. (a) Trajectory of the failed control experiment "from P1 to P2": black solid. Gray solid: stable cycles P1 and P2. Bottom-center: zoom into P2. Top-right insert: trajectory for the same range of *Per1* and *Per2* as in Figures 8c and 9. Top-left insert: Poincaré section of (*Per1*, *Per2*) at CLK=0.675. (b) Trajectory of the failed control experiment "from P1 to USS": black solid. Gray solid: P1, open dot: USS. Top-right insert: zoom into UP.

values of the unstable stationary point z_I^{USS}, and the remaining 14 variables are calculated by the ODEs with an initial state on P1. Again we found that the total system converged to the unstable stationary point z^{USS} and remained there, stably, by the control of the feedback vertex set I, only.

Deviating from the safe feedback vertex protocol of theorems 1.3 and 1.6, we found that the *reduced feedback vertex set*

$$\begin{aligned} I_* : &= I \setminus \{\text{CLK}\} \\ &= \{\text{PER1, PER2, CRY1, CRY2, RORc, CLK/BMAL1}\} \end{aligned} \tag{7.1}$$

is actually sufficient, when clamped, to control the remaining network on $\Gamma \setminus I_*$, even though $\Gamma \setminus I_*$ contains a 2-loop CLK $\leftrightarrow$ BMAL1.

We conclude that controlling the reduced feedback vertex set I_* is indeed

sufficient to control the total system, even when the target state is unstable originally. We give a mathematical reason for this surprising fact in section 7.4.

We next examined whether the system can be controlled equally well by a further reduction of vertices. We control only 5 among the 6 variables of I_* and try to control the system "from P1 to P2". We prescribed the forward time tracks $z_{I'}^{\mathrm{P2}}(t)$, $I' = \{$PER1, PER2, CRY1, CRY2, RORc$\}$. The dynamics of the remaining 16 variables, including the omitted informative nodes CLK and CLK/BMAL1, are calculated by ODEs with an initial state on P1. The result is shown in Figure 10: the trajectory converged to an unknown spurious quasiperiodic oscillation, and not to P2. Similarly we performed numerical experiments "from P2 to P1", "from P1 to UP" and "from P1 to USS". The control of the system succeeded in the cases "from P2 to P1", "from P1 to UP", and failed in the case "from P1 to USS". This demonstrates that controlling a non-informative set I' of feedback vertices set may fail to control the system.

We caution our reader that the above results do depend on the choice of prescribed variables. Controlling the forward time tracks $z_{I"}(t)$ of the 5 variables $I" = \{$PER1, CRY1, CRY2, RORc, CLK/BMAL1$\}$ among the 6 informative variables, for example, we can again control the dynamics of the whole system. In [Mo&al13], on the other hand, we observe how the 6 variables $I^* = \{$PER1, PER2, CRY1, CRY2, RORc, BMAL1$\}$ fail to control the remaining variables in three out of the four above protocols, even though $I^* \cup \{$CLK$\}$ also is a minimal feedback vertex set.

Our experiments demonstrate that even the reduced feedback vertex set I_* is a sufficient set to control the whole regulatory network. Our result provides a rational criterion to select variables if we aim at efficient open loop control of complex systems which involve many variables. It is quite powerful for biological systems, because biological systems are usually very complex: in many cases the regulatory edges are the only available information. Recent life sciences are aiming at the control of biological system for medical purposes. The problems of circadian rhythms in human, for example, cause physiological or mental diseases, including sleep difficulty or depression. Such problems may be solved if we succeed to control the activities of some genes. Of course it will remain impossible to control all molecules in a circadian rhythm system. Thus we have to select minimal but sufficient sets of accessible molecules

to control the system. Our theory may contribute to this ambitious goal, providing a rational criterion to identify key controlling molecules based on the graph information of their regulatory edges, alone.

7.4 Reduced feedback vertex sets

In this section we discuss the specific mathematical reason why the reduced feedback vertex set I_* of (7.1) was sufficient to control the remaining regulatory network $\Gamma\smallsetminus I_*$ when clamped to an existing solution $z_{I_*}(t)$.

Let J denote any set of vertices, not necessarily of feedback vertex type. We clamp variables $z_J^*(t)$ on J to a known solution $z^*(t) = (z_J^*(t), z_{\Gamma\smallsetminus J}^*(t))$ of the full network Γ. This is best described by a splitting of variables

$$\begin{aligned} \dot z_J &= F_J(z_J, z_{\Gamma\smallsetminus J})\,, \\ \dot z_{\Gamma\smallsetminus J} &= F_{\Gamma\smallsetminus J}(z_J, z_{\Gamma\smallsetminus J})\,. \end{aligned} \tag{7.2}$$

with suitable nonlinearities F_J, $F_{\Gamma\smallsetminus J}$. The trajectories $\zeta(t)$ of the remaining network $\Gamma\smallsetminus J$ then satisfy

$$\dot\zeta = F_{\Gamma\smallsetminus J}(z_J^*(t), \zeta)\,. \tag{7.3}$$

Note that (7.3) is a nonautonomously forced regulatory network, as in (1.1), on the remaining graph $\Gamma\smallsetminus J$, which has all vertices J deleted along with all edges oriented from or towards J. Forcing comes from the clamped variables $z_J^*(t)$. By assumption, $\zeta(t) := z_{\Gamma\smallsetminus J}^*(t)$ is a particular solution of the remaining network (7.3).

For example, first suppose $J = I$ is indeed a full feedback vertex set. Then $\Gamma\smallsetminus J$ is acyclic, hence with empty feedback vertex set. Therefore theorem 1.3 implies

$$\zeta(t) - z_{\Gamma\smallsetminus J}^*(t) \underset{t\to+\infty}{\longrightarrow} 0\,, \tag{7.4}$$

for any solution $\zeta(t)$ of (7.3). Therefore clamping a full feedback vertex set I controls all remaining variables $\zeta(t)$ to eventually follow the reference solution $z_{\Gamma\smallsetminus J}^*(t)$.

In the circadian section 7.3, however, we clamped only a reduced feedback vertex set $J = I_* = I\smallsetminus\{\mathrm{CLK}\}$. Still we were able to control all remaining

variables $z_{\Gamma \setminus J}$, including CLK itself. We now give a mathematical reason for that phenomenon, based on the network graph of Figure 8 and, as well, on the specific form of the nonlinearities of our simulation, as given in the appendix. Indeed the network alone cannot reveal such insight, in view of the only-if-part of theorem 1.3.

We first observe, by Figure 8, that the variables RORc, CLK/BMAL1, *Clk*, and *Bmal1* can be assumed to be given. Indeed the subsystem of CLK and BMAL1 does not feed back into those feed variables, except through the known clamped variable CLK/BMAL1 of I_*. We can therefore rewrite the subsystem for $C :=$ CLK and $B :=$ BMAL1 as

$$\begin{array}{rcccccc} \dot{B} & = & \beta(t) & - & aBC & - & k_B B \\ \dot{C} & = & \gamma(t) & - & aBC & - & k_C C \end{array} \tag{7.5}$$

with obvious abbreviations for $a, \beta(t), \gamma(t), k_B, k_C$; see (9.15), (9.14). Note $a, k_B, k_C, B, C > 0$. As in the proof of lemma 3.2, the differences $(b, c) := (\widetilde{B}, \widetilde{C}) - (B, C)$ of any two solutions of (7.5) satisfy a similar nonautonomous linear system

$$\begin{array}{rcccc} \dot{b} & = & -(a\hat{C}(t) + k_B)b & - & a\hat{B}(t)c \\ \dot{c} & = & -(a\hat{B}(t) + k_C)c & - & a\hat{C}(t)b \end{array} \tag{7.6}$$

The coefficients $\hat{B}(t), \hat{C}(t)$ are positive and uniformly bounded, interpolating between positive solutions B, C and $\widetilde{B}, \widetilde{C}$.

To show control $z(t) - z^*(t) \to 0$ for $t \to +\infty$, as before, we only have to show $b, c \to 0$. First suppose $b, c > 0$ for all $t \geq 0$. Then $\dot{b}, \dot{c} < 0$, by (7.6), implies monotone decay. Hence the limits

$$\lim_{t \to +\infty} b(t) = b_\infty \geq 0, \qquad \lim_{t \to +\infty} c(t) = c_\infty \geq 0 \tag{7.7}$$

exist. Positivity contradicts (7.6); hence $b_\infty = c_\infty = 0$. In case $b, c < 0$ we argue for the solution $-(b, c)$, analogously.

Next consider the case $b > 0 = c$, for some $t_0 > 0$ (again with completely analogous symmetric cases $b < 0 = c$, $b = 0 < c$, $b = 0 > c$, which we omit). Then $\dot{c}(t_0) < 0$ implies $b > 0 > c$ immediately afterwards, and for all $t > t_0$. Let us therefore consider the case $b > 0 > c$ (omitting $b < 0 < c$). Then

$b - c > 0$ and $\frac{d}{dt}(b-c) = -k_B b + k_C c < 0$ successively imply

$$\begin{array}{rcl} \lim_{t\to+\infty}(b(t)-c(t)) & = & 0\,, \qquad \text{and} \\ \lim_{t\to+\infty} b(t) & = & \lim_{t\to+\infty} c(t) \;=\; 0\,. \end{array} \tag{7.8}$$

This proves control (7.4) by clamping the circadian model at the reduced feedback vertex set $I_* := I \smallsetminus \{\mathrm{CLK}\}$, only. Our analysis confirms the numerical observations of section 7.3.

8 Discussion

We conclude the paper with a discussion of the scope and perspectives of our results. We review some further examples in section 8.1. Collecting caveats on the limitation of our approach, in 8.2, we happily proceed to generalize in 8.3. Section 8.4 indicates a few further areas of applications and we summarize our conclusions in 8.5.

8.1 Further examples

As further examples we discuss the damped harmonic oscillator, some simple chemical reaction networks, and the slightly more restrictive class of gene regulatory networks studied in [MoSa10].

In section 5.1 we have seen how an empty informative set $I = \varnothing$, i.e. absence of directed cycles, implies convergence to the unique globally asymptotically stable stationary solution. The linear Frobenius example of section 5.5, on the other hand, has already indicated some of the high-dimensional quasiperiodic complications to be encountered, even when the informative set I contains but one single element. The planar example of a single 2-cycle loop in section 5.3 and the Lorenz equations of section 5.4 have revealed some of the nonlinear dynamics complications which may arise for $|I| = 1$. We also recall the formidable ascidean network of section 7, where $|I| = 1$.

It is tempting, perhaps, to seek a further reduction of the *damped harmonic oscillator*

$$\ddot{z} + 2\nu\dot{z} + \omega^2 z = 0 \tag{8.1}$$

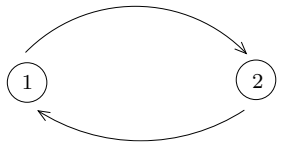

Figure 11: Regulatory graph of the damped harmonic oscillator. Note the negative feedback from vertex 1 to vertex 2 for negative discriminant $\nu^2 - w^2$.

to an empty feedback vertex set, because global asymptotic stability of $z \equiv 0$ prevails, for any $\nu > 0$. The equivalent system

$$\begin{aligned} \dot{z}_1 &= z_2 \qquad\qquad -\nu z_1 \\ \dot{z}_2 &= (\nu^2 - \omega^2) z_1 - \nu z_2 \end{aligned} \tag{8.2}$$

is a regulatory network which consists of a single loop of length 2; see section 5.3.
Negative discriminant, $\nu^2 < \omega^2$ implies negative feedback along the cycle; see Figure 11. We have already indicated in (1.6) how any negative self-feedback of vertex k can be incorporated into the negative feedback condition $\partial_1 F_k < 0$. It would be quite mistaken, however, to seek such a generalization of the present example and expect an empty informative set $I = \varnothing$, in general. Indeed consider the nonautonomous case $\omega^2 = (\omega(t))^2$ where the proper frequency is allowed to depend on time, periodically. It is well-known that $z \equiv 0$ can be destabilized by suitable choices of $\omega(t) > 0$. Indeed this is how children destabilize the boring rest state of a swing by raising and lowering their center of gravity at twice the swing's proper frequency. See for example the study of the Mathieu equation and related destabilization phenomena in [Arn73].

As a second example we briefly indicate how to subsume *chemical reaction networks* under the class of autonomous regulatory networks (1.3). First let us consider a simple reaction step

$$Z_1 + Z_2 \longrightarrow Z_3 + Z_4\,, \tag{8.3}$$

where Z_j indicate chemical substances with concentrations z_j. Assuming

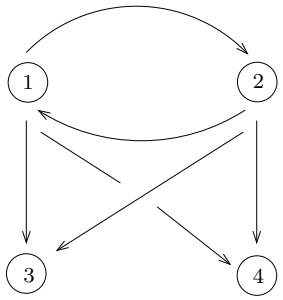

Figure 12: The regulatory graph contributed by a chemical reaction $Z_1 + Z_2 \longrightarrow Z_3 + Z_4$ see (8.3), (8.4).

decay and/or dilution rates d_j of z_j we obtain

$$\begin{aligned} \dot{z}_1 &= \ldots - \boldsymbol{k}(z_1, z_2) - d_1 z_1 \\ \dot{z}_2 &= \ldots - \boldsymbol{k}(z_1, z_2) - d_2 z_2 \\ \dot{z}_3 &= \ldots + \boldsymbol{k}(z_1, z_2) - d_3 z_3 \\ \dot{z}_4 &= \ldots + \boldsymbol{k}(z_1, z_2) - d_4 z_4 \end{aligned} \tag{8.4}$$

if we omit contributions of other reactions in the network. The reaction kinetics $\boldsymbol{k}(z_1, z_2)$ can still be chosen arbitrarily. Examples are mass action kinetics $\boldsymbol{k} = \kappa z_1 z_2$ or Michaelis-Menten terms $\boldsymbol{k} = \kappa z_1 z_2/(1 + \kappa_1 z_1 + \kappa_2 z_2)$. See Figure 12 for the contribution of this reaction to the total regulatory network. Here we assume $z_j > 0$ and $\partial_1 \boldsymbol{k}$, $\partial_2 \boldsymbol{k} > 0$ to omit self-loops at vertices 1 and 2. Note the 2-cycle $1 \longleftrightarrow 2$. If Figure 12 is the complete reaction network, we need informative sets I of a single vertex from $\{1, 2\}$, for the single forward reaction (8.3).

The reverse reaction of (8.3) will contribute another 2-cycle $3 \longleftrightarrow 4$ to the graph, analogously. In fact the resulting graph will be the complete bi-directional graph with four vertices. Reversible reactions therefore require and accommodate any choice of three vertices. More realistic networks and appropriately more intricate regulatory graphs can be built accordingly, and will be able to accommodate very general reaction rate expressions.

To be a little more specific consider the simple catalytic reaction step

$$Z_1 + Z_2 \longrightarrow Z_1 + Z_3 \tag{8.5}$$

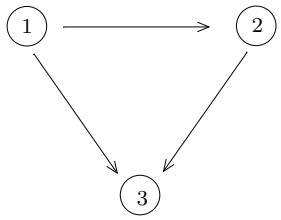

Figure 13: The regulatory graph autocatalytic chemical reaction $Z_1 + Z_2 \longrightarrow Z_1 + Z_3$; see (8.5), (8.6).

with decay/dilution and constant feeds $a_1, a_2 > 0$ of the inputs Z_1, Z_2. Then

$$\begin{aligned} \dot{z}_1 &= a_1 \qquad\qquad -d_1 z_1 \\ \dot{z}_2 &= a_2 - \boldsymbol{k}(z_1, z_2) - d_2 z_2 \\ \dot{z}_3 &= \qquad \boldsymbol{k}(z_1, z_2) - d_3 z_3 \end{aligned} \tag{8.6}$$

See Figure 13 for the regulatory graph of (8.5), (8.6) under the above monotonicity assumption on the quite general reaction rate $\boldsymbol{k}(z_1, z_2)$. Since the regulatory graph is acyclic, the informative set is empty and global convergence to the unique equilibrium, for $t \to +\infty$ ensues. Of course this is also evident from the ODE (8.6). Indeed $z_1 \to z_1^* := a_1/d_1$ implies $z_2 \to z_2^*$ with $0 = a_2 - \boldsymbol{k}(z_1^*, z_2^*) - d_2 z_2^*$ and hence $z_3 \to z_3^* := \boldsymbol{k}(z_1^*, z_2^*)/d_3$.
As a third example we return to the slightly more specific form

$$\dot{z}_k = f_k(t, z_{I_k}) - d_k(t) z_k \,, \tag{8.7}$$

$k = 1, \ldots, N$, of regulatory networks originally discussed by [Mo08, MoSa10]. For dissipativeness we assume all $f_k, \partial_z f_k \in C^0$ to be uniformly bounded and $d_k > 0$ to possess unbounded integrals

$$\int_{-\infty}^{t} d_k = +\infty \,, \tag{8.8}$$

for all $t \in \mathbb{R}$. Suppose $z_k(t)$ are known for all $t \in \mathbb{R}$ and all k in an informative set I. We choose an ordered labeling such that $I = \{N' + 1, \ldots, N\}$ and $I_{n'} \subseteq I \cup \{1, \ldots, n' - 1\}$; see lemma 2.2. We can then explicitly determine the noninformative forward time tracks $z_{n'}(t)$, $t \in \mathbb{R}$, $n' = 1, \ldots, N'$, of globally bounded solutions $z(t)$, $t \in \mathbb{R}$, by induction over n'. Indeed fix

$t_0 \in \mathbb{R}$ arbitrarily and invoke variations-of-constants with the abbreviation $\varphi_k(t) := f_n(t, z_{I_k}(t))$ in

$$\dot{z}_k(t) = \varphi_k(t) - d_k(t) z_k(t) \tag{8.9}$$

to obtain

$$\begin{aligned} z_{n'}(t) = \exp\left(-\int_{t_0}^{t} d_{n'}(s)ds\right) z_{n'}(t_0) + \\ + \int_0^{t-t_0} \exp\left(-\int_{t-s}^{t} d_{n'}(\sigma)d\sigma\right) \varphi_{n'}(t-s)ds \end{aligned} \tag{8.10}$$

for all $n' = 1, \ldots, N'$ and all $t \in \mathbb{R}$. For $t_0 \to -\infty$, boundedness of z on $\mathbb{R}$ and assumption (8.8) imply

$$z_{n'}(t) = \int_0^{+\infty} \exp\left(-\int_{t-s}^{t} d_{n'}(\sigma)d\sigma\right) \varphi_{n'}(t-s)ds. \tag{8.11}$$

Because $\varphi_{n'}(t)$ depends only on $z_k(t)$ with $k \in I_{n'} \subseteq \{1, \ldots, n'-1\}$, by lemma 2.2, equation (8.11) is an explicit recursive formula for $n' = 1, \ldots, N'$ which determines all the complementary nodes from the informative data. In the autonomous case, (8.11) is an explicit expression which inverts the injective projection $\mathcal{P}_I z(0) := z_I(\cdot)$ of theorem 1.6 for $z(0)$ in the global attractor $\mathcal{A}$.

If informative forward time tracks $z_I(t)$ are not known globally, but only on sufficiently long intervals $0 \leq t \leq T$, then (8.10) with $t_0 = 0$ provides a recursion with exponential error estimates of order

$$\exp(-\delta T), \tag{8.12}$$

for $z_{n'}(T)$, provided that all remaining $d_{n'}(t)$ are uniformly positive and

$$\inf_t d_{n'}(t) > \delta > 0 \tag{8.13}$$

for all $n' = 1, \ldots, N'$. The same exponential error estimate (8.12) holds for general regulatory networks (1.1) provided that

$$\inf_{t,z} -\partial_1 F_{n'}(t, z_{n'}, z_{I_{n'}}) > \delta > 0\,, \tag{8.14}$$

by analogous arguments. Due to the nonlinear dependence of $F_{n'}$ on $z_{n'}$, however, we lack an explicit recursive expression like (8.11) for the bounded solutions $z_{n'}(t)$ on the remaining nodes.

8.2 Caveats

We recall and outline some limitations of our results. We address determination of the informative set I, its necessity for being determining, and we caution against mistaking I as a dimension reduction.

Our first caveat concerns the *determination of the informative vertex set* I of the regulatory di-graph Γ, which in turn provides the determining nodes for the regulatory ODE (1.1). By corollary 2.4 the informative set I is a feedback vertex set of Γ, intercepting all directed cycles. Deciding on existence and finding k-element feedback vertex sets of a di-graph Γ is long known to be NP-complete in the number N of vertices. See [Ka75], and for more recent progress [Ch&al08]. As regulatory networks get more complex, then, the mere task of identifying suitable sets I of determining nodes may become a practical obstacle, eventually. In the modest examples presented here this task could still be settled bare-handedly. In fact the accessibility of data should play a more important role for the selection of the informative set I, in actual experiments, than complexity or minimality considerations on the feedback vertex set I. Redundancy of I may indeed be a welcome tool to cross-check results and to indicate possible errors in the hypothesized regulatory network itself.

A second caveat concerns *necessity of the full informative set* I, to be determining. The example of a mammal circadian regulatory network in sections 7.3 and 7.4 has already indicated that a small enough subset I' of a minimal informative set I may fail to determine the asymptotics of specific reference solutions, even when I' has been clamped to follow that reference solution precisely. The opposite phenomenon appears in our proof of the only-if-part of theorem 1.3, in a slightly different guise; see section 6. To show that a determining set I is necessarily informative, alias a feedback vertex set, it is not sufficient to just require I to be determining for a fixed regulatory ODE manifestation of the di-graph Γ by a choice of nonlinearities F_k. It was actually necessary to require I to be determining for *all* choices of F_k. It is therefore not too surprising that smaller subsets I' of I, which are not informative, may still be determining on some specific occasions. If we seek determining nodes of a complex regulatory network based on its di-graph Γ, only, and without additional modeling information on F_k, then the full

feedback vertex sets alias informative sets I are the monitors of choice.

Naive application of *Takens embedding* [Ta10] would claim attractor reconstruction by monitoring the time track $z_k(t)$ of just a single vertex k. Of course such a naive approach is not warranted by the genericity requirements of the actual Takens embedding theorem. Indeed it patently fails, for example, at any input vertex k with empty predecessor set I_k of any regulatory network (1.3) with nontrivial dynamics: while $z_k(t)$ tends to the same constant, for all initial conditions, $z(t)$ does not. Of course that failure is due to an inappropriate choice of the monitoring vertex.

It may still be possible, however, to reconstruct the global attractor $\mathcal{A}$ from observations on one or very few suitably chosen single nodes k, in generic situations. Under mild assumptions on the network graph, Joly [Jo11] has in fact shown how stationary and periodic solutions can be reconstructed from the time track of just a *single node*. His main assumption is C^1 genericity of the regulatory functions which define the network. For a precursor result under more restrictive assumptions on the graph Γ see also [Go&al10].

Genericity is an abstract assumption rather than a concrete one: reconstruction works for nonlinearities F_k in some abstract set of large Baire category, viz. a countable intersection of sets each of which is open and dense. On the downside, C^1 genericity might mean that the result fails for all nonlinearities of differentiability class C^2. More importantly, and more realistically, the assumption will exclude the biologically relevant switching behavior where some nonlinearities become independent of some of their inputs, in certain open regions of phase space. Indeed such switching may locally undermine the underlying graph structure exploited globally for the beautiful genericity result of Joly.

To illustrate genericity we only discuss a linear example here. Consider a diagonalizable $N \times N$ matrix C with distinct eigenvalues $\lambda_j \in \mathbb{C}$ and eigenvectors z^j. Generically we may also assume all non-diagonal entries of C to be nonzero, and all components z^j_k of all eigenvectors to be nonzero, likewise. Then

$$\dot{z} = Cz - z \tag{8.15}$$

is a regulatory network with at least the complete graph contained in the network graph Γ. Diagonal elements $c_{kk} \geq 1$ of C will add self-loops. Any

minimal feedback vertex set I therefore contains at least $N-1$ elements. On the other hand the time track $z_k(t)$ of any single vertex k will be sufficient to faithfully reconstruct $z(t)$, in this generic situation. This is reminiscent of the Frobenius example of section 5.5 in (5.16), (5.17), where the single vertex N was determining.

Additional special structures of the regulatory network may also assist in attractor reconstruction from orbits other than the feedback vertex set. The Lorenz system (5.10) of section 5.4, for example, also allows reconstruction from $z_1(t)$, $t \in \mathbb{R}_-$, even though $I = \{2\}$ is the only minimal feedback vertex set. Indeed (5.10) implies that the determining time track $z_2 = z_1 + \dot{z}_1/\sigma$ is also known, once z_1 is. With slightly more effort z_1, and hence z_2, can also be reconstructed from $z_3(t)$, $t \in \mathbb{R}_-$, on the global attractor.

Neither the genericity result [Jo11] nor these examples contradict the only-if-part of theorem 1.3. Our result holds for all nonlinearities, not only some particular or many unspecified "generic" ones. These, and many other, objections notwithstanding it remains important to welcome, to explore, and to further clarify the elegant Takens embedding approach and its intriguing interaction with the network topology.

Our third caveat concerns *dimension reduction*. In PDEs, viz. in dynamics in infinite dimensions, the question of a reduction of the dynamics on finite-dimensional global attractors to an ODE has been thoroughly investigated under the name of inertial manifolds; see for example [MPSe87, Co&al89, FoTi91, Ed&al94, SeYo02] and others. Even in finite dimensional ODEs like our regulatory networks a reduction of dimensions is always welcome. We caution our reader, however, that we do not claim a reduction to any ODE on the informative set I. Again, the linear Frobenius case of section 5.5 provides an autonomous counterexample: even though $I = \{N\}$ is a singleton, periodic and quasiperiodic solutions do arise.

In general, knowledge of only an initial condition $z_I(0)$ on the feedback vertex set I is not sufficient to determine the full history time track $z_I(t),\ t \in \mathbb{R}_-$. But only when that history time track is known, theorem 1.6 asserts the reconstruction of $z(0)$, and hence of the full time track $z(t)$ on the global attractor.

For stationary solutions, only, the initial condition $z_I(0)$ on the feedback vertex set determines the full (constant) history time track $z_I(t),\ t \in \mathbb{R}_-$. In

that very special case, a dimension reduction to a closed equilibrium equation involving only the feedback vertex variables z_I is possible. See [Mo&al13] for further details.

In the next section we will argue, however, that a reduction to an ODE on the cyclicity set C of regulatory networks, i.e. to the union of all vertices on di-cycles, is possible for the global attractor, also in the nonstationary case.

8.3 Generalizations

We briefly comment on five topics which involve adaptations and generalizations of the elementary results presented here. We begin with the question of dimension reduction raised at the end of the previous section. We then comment on the cases of discrete time as well as vector-valued and PDE settings. Moving on to nonautonomous aspects we briefly mention stochastic perturbations.

Consider the autonomous version (1.3) of a connected regulatory network Γ under the assumptions of the global attractor theorem 1.6. For *dimension reduction* on the global attractor $\mathcal{A}$ let C_0 denote the cyclicity set of the di-graph Γ, i.e. the set of all vertices which lie on di-cycles of length at least two, or possess self-loops. For simplicity we first assume C_0 to be strongly connected, i.e. C_0 contains directed paths, in either direction, between any two vertices of C_0. Collapsing C_0 to a single vertex without self-loop, for a moment, we can then decompose the vertices of Γ disjointly into

$$\{1, \dots, N\} = C_- \cup C_0 \cup C_+ \tag{8.16}$$

such that C_- are the predecessors and C_+ the successors of C_0 in the resulting acyclic graph. In other words there exists a directed path from any element of C_- to some suitable element of C_0, and from some suitable element of C to any element of C_+. Because C_0 is assumed to be strongly connected, exactly one of these alternatives holds for any vertex outside C_0. In particular induction shows that $z_{C_-}(t)$ converges to a unique equilibrium because $I_{C_-} = \varnothing$ on the autonomous acyclic predecessor subgraph C_-. Substituting this equilibrium for values of z_{C_-} which occur in inputs I_k of $k \in C_0$, we obtain an autonomous reduced ODE

$$\dot{z}_k = \widetilde{F}_k(z_k, z_{I_k \cap C_0}) \tag{8.17}$$

for k in the cyclicity set C_0.

To show that the successor variable z_{C_+} is in fact enslaved by the cyclicity variables z_{C_0} on the global attractor $\mathcal{A}$, i.e.

$$z_{C_+} = \Phi(z_{C_0}) \tag{8.18}$$

for a suitable function $\Phi : \mathbb{R}^{|C_0|} \to \mathbb{R}^{|C_+|}$ we invoke theorem 1.6. Indeed let $z(0) \in \mathcal{A}$ be in the global attractor. Then the unique bounded solution $z_{C_0}(t)$, $t \in \mathbb{R}_-$ of (8.17) with initial condition $z_{C_0}(0)$ determines $z_I(\cdot)$ provided we choose the informative set I to be a subset of the cyclicity set C_0, without loss of generality. But injectivity (1.14) then implies uniqueness of $z(0)$, and in particular of $z_{C_+}(0)$. Now define the mapping $\Phi(z_{C_0}(0)) := z_{C_+}(0)$ to complete the proof of the dimension reduction (8.17), (8.18) to the connected cyclicity set C_0.

The connected cyclicity set of the ascidian network in section 7.1, Figure 5, with a singleton informative set is given in Figure 6.

The cyclicity set C_0 may not be connected, in general. Collapsing each connected component of C_0 to a separate single vertex, then, we obtain a disjoint Morse type decomposition of Γ into

$$\{1, \ldots, N\} = C_- \cup C_0 \cup H \cup C_+ \,, \tag{8.19}$$

as we explain next; see also [Ara&al09]. Here the cyclicity set C_0 can be decomposed into its disjoint strongly connected components

$$C_0 = C_1 \cup \ldots \cup C_m \,. \tag{8.20}$$

We label the components C_j of C_0 such that any oriented path through any vertex $k \in H$ can be extended to hit cyclicity components C_{j_-}, before k, and C_{j_+}, after k, only if $j_- < j_+$. In other words the labeling C_j is compatible with the partial order associated to the acyclic di-graph with individually collapsed C_j. The vertices in C_- precede all cyclicity, as before, and the vertices in C_+ are the ultimate successors.

Our previous arguments then apply inductively over $j = 1, \ldots, m$, to recover a reduction (8.17) of the dynamics on the global attractor $\mathcal{A}$ to an ODE on z_{C_0}. Again $z_{C_-}(t)$ tends to equilibrium on the ultimate predecessors. Enslaving (8.18) extends to all remaining variables:

$$z_{H \cup C_+} = \Phi(z_{C_0}) \,. \tag{8.21}$$

More precisely, in fact, z_k is enslaved already by only those z_{C_j} for which the "vertex" C_j precedes k in the acyclic collapsed regulatory graph. A similar skew-product structure of predecession holds for the reduced ODE (8.17) on the cyclicity set.

We plan to elaborate on such generalizations elsewhere in the context of suitable applications. The topic of dimension reduction is indeed critical for "model-free" representations of dynamics, for example via Takens embedding [Ta10]: the required amount of data to accurately model the dynamics on the global attractor grows exponentially with the dimension of $\mathcal{A}$ itself, and a conservative bound on that dimension is the size $|C_0|$ of the cyclicity set.

Of course our results can be adapted to discrete time iterations

$$z_k^{n+1} = F_k^n(z_k^n, z_{I_k}^n)\,, \tag{8.22}$$

$n \in \mathbb{Z}$, of regulatory networks. Dissipativeness extends to discrete time; a sufficient condition to replace (1.4) would be a decrease of Euclidean norm

$$\sum_{k=1}^{N} z_k^T F_k^n(z_k, z_{I_k}) < |z|_2^2\,, \tag{8.23}$$

uniformly for all integer n and for large $|z|_2$. Similarly, the decay condition (1.5) translates into

$$|\partial_1 F_k^n(z_k, z_{I_k})| < 1 \tag{8.24}$$

uniformly for all $n \in \mathbb{Z}$, $k = 1, \ldots, N$ and $z \in \mathbb{R}^N$. The autonomous case $F_k^n = F_k$ requires the nonlinearities not to depend on the iterator variable n, explicitly. Note that prehistories exist on the autonomous global attractor $\mathcal{A}$ due to its construction as the ω-limit set of a large ball. Invertibility of (8.22) to provide a *unique* extension in backwards time is not required.

Similarly our results extend to the ODE *vector case* $z_k \in \mathbb{R}^{m_k}$ of total dimension $m = m_1 + \ldots + m_N$. A straightforward condition for dissipativeness to replace (1.4), based on a decreasing Euclidean norm $|z(t)|_2$, would be

$$\sum_{k=1}^{N} z_k^T F_k(t, z_{k,I_k}) < 0\,, \tag{8.25}$$

uniformly for $t \in \mathbb{R}$ and large $|z|_2$. A sufficient decay condition to replace (1.5) is

$$\partial_1 F_k(t, z_k, z_{I_k}) < 0\,, \tag{8.26}$$

uniformly for all $t \in \mathbb{R}$, $k = 1, \dots, N$ and bounded $z \in \mathbb{R}^m$. Here (8.26) indicates that the quadratic form of the Jacobian $m_k \times m_k$ matrix $\partial_1 F_k$ with respect to the first entry z_k is to be strictly negative definite.

Similarly our results apply to*PDE extensions* of reaction-diffusion type, e.g. of the form

$$z_{k,t} = D_k \Delta_x z_k + F_k(t, x, z_k, z_{I_k})\,, \tag{8.27}$$

under appropriate conditions. The operators $D_k\Delta + \partial_1 F_k(t, \cdot, z_k(\cdot), z_{I_k}\cdot)$ for example, should be negative definite. Here $\partial_1 F_k$ again indicates the partial derivatives with respect to the first occurrence of z_k, and the arguments $z_k(\cdot)$, $z_{I_k}(\cdot)$ are arbitrary functions of x in the region Ω of the x-Laplacian Δ_x, in the appropriate Sobolev space. Note however that the present reduction requires, and stops at, a full profile $(t, x) \mapsto z_I(t, x)$ of the informative components, both in $t \in \mathbb{R}_-$ and $x \in \Omega$. Just like the PDE dimension reductions discusssed above, a further reduction of the determining profiles $z_I(t, \cdot)$ to finitely many nodes or finitely many modes in x, e.g. in the spirit of [HaRa03], requires additional analysis which we do not pursue here.

The effects of *stochastic perturbations* are closely linked to nonautonomous effects. Indeed additive and parametric noise as well as the skew product structure of stochastic cocycles [Arn98, KlRa11], can be subsumed under a regulatory network structure

$$\dot{z}_k = F_k(\omega, t, z_k, z_{I_k}) \tag{8.28}$$

where $\omega \in \Omega$ fixes the specific variant of the nonlinearities F_k in some suitable probability space Ω.

Here we assume that the overall directed graph Γ itself is not subject to stochastic fluctuations of its regulatory predecessor structure I_k. Likewise we assume that dissipativity like (1.5) remains valid, uniformly for all stochastic instances $\omega \in \Omega$. Then theorem 1.3 remains valid in the stochastic setting, for each choice of ω: any feedback vertex set I indeed remains a set of determining nodes which faithfully represents the dynamics $z(t)$ of the stochastic

regulatory network, asymptotically for $t \to +\infty$. Of course this easy and direct observation does not replace an in-depth stochastic analysis of asymptotic expectations, variances, or the robustness of the regulatory tasks of the network itself.

8.4 Further applications

We have mentioned chemical reaction networks as another application area in section 8.1. We briefly glance at the wide fields of control, of chaos synchronization, and at neural and electrical networks here.

A most direct and heavily invasive approach towards *control* of regulatory network dynamics was already taken in section 7.3. In fact we have prescribed $z_I(t)$ on an informative feedback vertex set of the circadian regulatory network to follow a particular stable or unstable periodic or stationary reference solution $z^*(t)$ of the network. We observed how this was sufficient to enslave the whole network dynamic $z(t)$ to follow $z^*(t)$, asymptotically for $t \to +\infty$. Any open loop control of an originally autonomous regulatory network (1.3) in fact renders the network nonautonomous, as in (1.1). As in the stochastic case (8.28) of section 8.3, feedback vertex sets remain determining in the sense of theorem 1.3, as long as dissipativity and decay conditions remain intact. The success of open loop control also suggests a prominent role of feedback vertex sets as a target for more sophisticated closed loop feedback control schemes in regulatory networks. For example it seems advisable, whenever practically feasible, to rely on a prudently chosen feedback vertex set I for a set of observables $z_I(t)$ to monitor the state of the regulatory network. Likewise, input to the feedback vertex variable ODEs $\dot{z}_i = \dots$ by actuator control variables $u(t)$ may prove efficient to control the entire network dynamics. We hope to further pursue feedback control via feedback vertex sets elsewhere.

The basic idea of *chaos synchronization* and the associated topic of signal encryption by chaotic oscillators are related to open loop control. For a simple example consider an autonomous dissipative regulatory network $\dot{z} = F(z)$ on $\mathbb{R}^N$ with decay condition and inherently chaotic dynamics, like the Lorenz system (5.10) of section 5.4. With two identical oscillators $z^1, z^2 \in \mathbb{R}^N$ we

may consider the first driving the second according to

$$\begin{aligned} \dot{z}^1 &= F(z^1) \\ \dot{z}^2 &= F(z^2) + D(z^1 - z^2) \end{aligned} \tag{8.29}$$

Suppose we consider diagonal driving matrices $D = \mathrm{diag}(d_1, \ldots, d_n)$ with diagonal entries $d_k = 0$ unless $k \in I$ is in a fixed chosen feedback vertex set I. For sufficiently large $d_k > 0$ on $k \in I$ this basically forces $z^2_I(t)$ to (almost) coincide with $z^1_I(t)$, on I and hence everywhere:

$$z^2(t) \approx z^1(t) \tag{8.30}$$

after some initial transients; see theorems 1.3 and 1.6. Thus the first oscillator z^1 forces z^2 into (almost) synchrony, even though the transmitted carrier signal $z_I(t)$ may appear chaotic. Refined versions of this idea include input signals to z^1 which, after encryption into the chaotic transmitted signal $z_I(t)$, are recovered from the full dynamics $z^2(t)$ of the second oscillator. See for example [PeCa98, Be&al04] for further details. Our present contribution is the systematic identification of the informative signal $z_I(t)$ to be transmitted: I should be a feedback vertex set of a regulatory network description of the chaotic oscillator $\dot{z} = F(z)$ by its associated di-graph Γ.

Applications of our results to neural and electrical networks are tempting. For simplicity let us consider a system of N not necessarily identical FitzHugh-Nagumo cells

$$\begin{aligned} \dot{z}^1_k &= f_k(z^1_k) - z^2_k + g_k(z^1_{I_k}) \,, \\ \dot{z}^2_k &= a_k(b_k z^1_k - c_k z^2_k) \,, \end{aligned} \tag{8.31}$$

$k = 1, \ldots, N$. See Figure 14 for a representation as a regulatory network. The predecessor or input subsets I_k of z^1_k define a di-graph structure Γ on the z^1-components, only. Choosing only z^1_k to represent feedback vertices, throughout the network, we see that feedback vertex sets of the coupling graph Γ of the nerve cells become feedback vertex sets to the entire regulatory network (8.31). Unfortunately the cubic nonlinearities f_k which generate the essential excitability feature of neurons also force self-loops at every vertex z^1_k of the network. This prevents further reduction to feedback vertex sets I which are strictly smaller than the entire network Γ. On the other hand

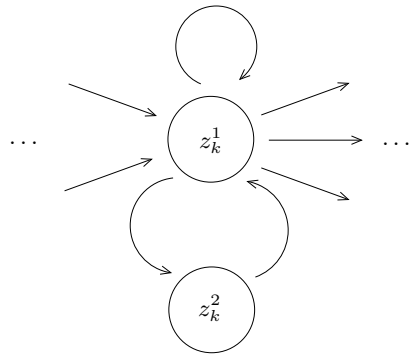

Figure 14: Motif of a neural regulatory network which represents a single cell of FitzHugh-Nagumo type. Self-coupling and neighbor coupling only occurs in the variable z_k^1.

neural networks provide an exciting field to further explore the idea of Morse decompositions of networks outlined in (8.19)–(8.21) above, albeit with the modification that the dynamics of individual vertices must accommodate more elaborate excitable dynamics.

Man-made systems like *electrical power networks* are designed with the goal of stability, quite contrary to the excitability property of neural networks. One issue here is the monitoring and control of deviations of the electrical phase z_k throughout the vertices $k = 1, \ldots, N$ of the network. We may represent the global coupling structure by a regulatory network di-graph Γ again. Assume local controllers to stabilize phase, locally. This amounts to a decay condition like (1.5). As a monitoring strategy we may then choose a feedback vertex set I and use informative $z_I(t)$ sensors as observables to carefully and faithfully represent the state $z(t)$ of the entire network. We may even select redundant informative sets to cross-check data and system reliability. This simple observation, based on theorem 1.3 again, may assist in the formidable task of designing flexible and "intelligent" power grids of our future.

8.5 Conclusion

Summarizing, our paper offers some progress towards a systematic understanding of the long-term dynamics of regulatory networks (1.1) via an as-

sociated di-graph Γ.

We have noticed the equivalence of the graph theoretic notions of informative and feedback vertex sets with the notion of determining vertex sets in long-term dynamics; see section 2 and theorem 1.3. In the autonomous case this also leads to a faithful reconstruction of the global attractor by time-tracks on any informative set; see theorem 1.6.

From an applications perspective, discussed in sections 7 and 8.4, we are confident that the notion of informative sets is crucial

(i) to decide where to measure,

(ii) to aid modeling,

(iii) to check for data consistency,

(iv) to control dynamical properties,

in rather general regulatory networks.

The control aspect, together with the hierarchy of network dependencies at the core of our Morse type decomposition of the di-graph Γ into cyclicity components, opens a rational approach towards an understanding of hierarchic modularity of regulatory networks. Indeed any cut of the di-graph Γ into two pieces or "units", where all vertices of the one precede those of the other, along edge direction, offers the possibility to view the preceding unit as controlling the dynamics of the other to an extent specified by the respective feedback vertex sets of those units.

9 Appendix

9.1 Model equations for mammalian circadian rhythm

The mathematical model which we used in Section 7.3 is written as a system of ODEs including 21 variables, $Per1$, $Per2$, $Cry1$, $Cry2$, *Rev-erb*α, Clk, $Bmal1$, $Rorc$, PER1, PER2, CRY1, CRY2, REV-ERBα, CLK, BMAL1, RORc, PER1/CRY1, PER2/CRY1, PER1/CRY2, PER2/CRY2 and CLK/BMAL1.

(9.1)

$$\frac{dPer1}{dt} = (V_{0,Per1} + V_{1,Per1}\frac{\text{CLK/BMAL1}^{na_{1,Per1}}}{KA_{1,Per1}^{na_{1,Per1}} + \text{CLK/BMAL1}^{na_{1,Per1}}})$$
$$* \frac{KI_{1,Per1}^{ni_{1,Per1}}}{KI_{1,Per1}^{ni_{1,Per1}} + \text{PER1/CRY1}^{ni_{1,Per1}}} * \frac{KI_{2,Per1}^{ni_{2,Per1}}}{KI_{2,Per1}^{ni_{2,Per1}} + \text{PER1/CRY2}^{ni_{2,Per1}}}$$
$$* \frac{KI_{3,Per1}^{ni_{3,Per1}}}{KI_{3,Per1}^{ni_{3,Per1}} + \text{PER2/CRY1}^{ni_{3,Per1}}} * \frac{KI_{4,Per1}^{ni_{4,Per1}}}{KI_{4,Per1}^{ni_{4,Per1}} + \text{PER2/CRY2}^{ni_{4,Per1}}}$$
$$- k_{m,Per1}Per1$$

(9.2)

$$\frac{dPer2}{dt} = (V_{0,Per2} + V_{1,Per2}\frac{\text{CLK/BMAL1}^{na_{1,Per2}}}{KA_{1,Per2}^{na_{1,Per2}} + \text{CLK/BMAL1}^{na_{1,Per2}}})$$
$$* \frac{KI_{1,Per2}^{ni_{1,Per2}}}{KI_{1,Per2}^{ni_{1,Per2}} + \text{PER1/CRY1}^{ni_{1,Per2}}} * \frac{KI_{2,Per2}^{ni_{2,Per2}}}{KI_{2,Per2}^{ni_{2,Per2}} + \text{PER1/CRY2}^{ni_{2,Per2}}}$$
$$* \frac{KI_{3,Per2}^{ni_{3,Per2}}}{KI_{3,Per2}^{ni_{3,Per2}} + \text{PER2/CRY1}^{ni_{3,Per2}}} * \frac{KI_{4,Per2}^{ni_{4,Per2}}}{KI_{4,Per2}^{ni_{4,Per2}} + \text{PER2/CRY2}^{ni_{4,Per2}}}$$
$$- k_{m,Per2}Per2$$

(9.3)

$$\frac{dCry1}{dt} = (V_{0,Cry1} + V_{1,Cry1}\frac{\text{CLK/BMAL1}^{na_{1,Cry1}}}{KA_{1,Cry1}^{na_{1,Cry1}} + \text{CLK/BMAL1}^{na_{1,Cry1}}} +$$
$$V_{2,Cry1}\frac{\text{RORc}^{na_{2,Cry1}}}{KA_{2,Cry1}^{na_{2,Cry1}} + \text{RORc}^{na_{2,Cry1}}}) * \frac{KI_{1,Cry1}^{ni_{1,Cry1}}}{KI_{1,Cry1}^{ni_{1,Cry1}} + \text{PER1/CRY1}^{ni_{1,Cry1}}}$$
$$* \frac{KI_{2,Cry1}^{ni_{2,Cry1}}}{KI_{2,Cry1}^{ni_{2,Cry1}} + \text{PER1/CRY2}^{ni_{2,Cry1}}} * \frac{KI_{3,Cry1}^{ni_{3,Cry1}}}{KI_{3,Cry1}^{ni_{3,Cry1}} + \text{PER2/CRY1}^{ni_{3,Cry1}}}$$
$$* \frac{KI_{4,Cry1}^{ni_{4,Cry1}}}{KI_{4,Cry1}^{ni_{4,Cry1}} + \text{PER2/CRY2}^{ni_{4,Cry1}}} * \frac{KI_{5,Cry1}^{ni_{5,Cry1}}}{KI_{5,Cry1}^{ni_{5,Cry1}} + \text{REV-ERB}\alpha^{ni_{5,Cry1}}}$$
$$- k_{m,Cry1}Cry1$$

(9.4)

$$\frac{dCry2}{dt} = (V_{0,Cry2} + V_{1,Cry2}\frac{\text{CLK/BMAL1}^{na_{1,Cry2}}}{KA_{1,Cry2}^{na_{1,Cry2}} + \text{CLK/BMAL1}^{na_{1,Cry2}}} + V_{2,Cry2}\frac{\text{RORc}^{na_{2,Cry2}}}{KA_{2,Cry2}^{na_{2,Cry2}} + \text{RORc}^{na_{2,Cry2}}}) * \frac{KI_{1,Cry2}^{ni_{1,Cry2}}}{KI_{1,Cry2}^{ni_{1,Cry2}} + \text{PER1/CRY1}^{ni_{1,Cry2}}} * \frac{KI_{2,Cry2}^{ni_{2,Cry2}}}{KI_{2,Cry2}^{ni_{2,Cry2}} + \text{PER1/CRY2}^{ni_{2,Cry2}}} * \frac{KI_{3,Cry2}^{ni_{3,Cry2}}}{KI_{3,Cry2}^{ni_{3,Cry2}} + \text{PER2/CRY1}^{ni_{3,Cry2}}} * \frac{KI_{4,Cry2}^{ni_{4,Cry2}}}{KI_{4,Cry2}^{ni_{4,Cry2}} + \text{PER2/CRY2}^{ni_{4,Cry2}}} * \frac{KI_{5,Cry2}^{ni_{5,Cry2}}}{KI_{5,Cry2}^{ni_{5,Cry2}} + \text{REV-ERB}\alpha^{ni_{5,Cry2}}} - k_{m,Cry2}Cry2$$

(9.5)

$$\frac{dRev\text{-}erb\alpha}{dt} = V_{1,Rev\text{-}erb\alpha}\frac{\text{CLK/BMAL1}^{na_{1,Rev\text{-}erb\alpha}}}{KA_{1,Rev\text{-}erb\alpha}^{na_{1,Rev\text{-}erb\alpha}} + \text{CLK/BMAL1}^{na_{1,Rev\text{-}erb\alpha}}} * \frac{KI_{1,Rev\text{-}erb\alpha}^{ni_{1,Rev\text{-}erb\alpha}}}{KI_{1,Rev\text{-}erb\alpha}^{ni_{1,Rev\text{-}erb\alpha}} + \text{PER1/CRY1}^{ni_{1,Rev\text{-}erb\alpha}}} * \frac{KI_{2,Rev\text{-}erb\alpha}^{ni_{2,Rev\text{-}erb\alpha}}}{KI_{2,Rev\text{-}erb\alpha}^{ni_{2,Rev\text{-}erb\alpha}} + \text{PER1/CRY2}^{ni_{2,Rev\text{-}erb\alpha}}} * \frac{KI_{3,Rev\text{-}erb\alpha}^{ni_{3,Rev\text{-}erb\alpha}}}{KI_{3,Rev\text{-}erb\alpha}^{ni_{3,Rev\text{-}erb\alpha}} + \text{PER2/CRY1}^{ni_{3,Rev\text{-}erb\alpha}}} * \frac{KI_{4,Rev\text{-}erb\alpha}^{ni_{4,Rev\text{-}erb\alpha}}}{KI_{4,Rev\text{-}erb\alpha}^{ni_{4,Rev\text{-}erb\alpha}} + \text{PER2/CRY2}^{ni_{4,Rev\text{-}erb\alpha}}} - k_{m,Rev\text{-}erb\alpha}Rev\text{-}erb\alpha$$

(9.6)

$$\frac{dClk}{dt} = (V_{0,Clk} + V_{1,Clk}\frac{\text{RORc}^{na_{1,Clk}}}{KA_{1,Clk}^{na_{1,Clk}} + \text{RORc}^{na_{1,Clk}}}) * \frac{KI_{1,Clk}^{ni_{1,Clk}}}{KI_{1,Clk}^{ni_{1,Clk}} + \text{REV-ERB}\alpha^{ni_{1,Clk}}} - k_{m,Clk}Clk$$

$$\frac{dBmal1}{dt} = (V_{0,Bmal1} + V_{1,Bmal1}\frac{\text{RORc}^{na_{1,Bmal1}}}{KA_{1,Bmal1}^{na_{1,Bmal1}} + \text{RORc}^{na_{1,Bmal1}}}) * \frac{KI_{1,Bmal1}^{ni_{1,Bmal1}}}{KI_{1,Bmal1}^{ni_{1,Bmal1}} + \text{REV-ERB}\alpha^{ni_{1,Bmal1}}} - k_{m,Bmal1}Bmal1 \tag{9.7}$$

(9.8)

$$\begin{aligned}\frac{dRorc}{dt} = (&V_{0,Rorc} + V_{1,Rorc}\frac{\text{CLK/BMAL1}^{na_{1,Rorc}}}{KA_{1,Rorc}^{na_{1,Rorc}} + \text{CLK/BMAL1}^{na_{1,Rorc}}} \\ &+ V_{2,Rorc}\frac{\text{RORc}^{na_{2,Rorc}}}{KA_{2,Rorc}^{na_{2,Rorc}} + \text{RORc}^{na_{2,Rorc}}}) \\ &* \frac{KI_{1,Rorc}^{ni_{1,Rorc}}}{KI_{1,Rorc}^{ni_{1,Rorc}} + \text{PER1/CRY1}^{ni_{1,Rorc}}} * \frac{KI_{2,Rorc}^{ni_{2,Rorc}}}{KI_{2,Rorc}^{ni_{2,Rorc}} + \text{PER1/CRY2}^{ni_{2,Rorc}}} \\ &* \frac{KI_{3,Rorc}^{ni_{3,Rorc}}}{KI_{3,Rorc}^{ni_{3,Rorc}} + \text{PER2/CRY1}^{ni_{3,Rorc}}} * \frac{KI_{4,Rorc}^{ni_{4,Rorc}}}{KI_{4,Rorc}^{ni_{4,Rorc}} + \text{PER2/CRY2}^{ni_{4,Rorc}}} \\ &* \frac{KI_{5,Rorc}^{ni_{5,Rorc}}}{KI_{5,Rorc}^{ni_{5,Rorc}} + \text{REV-ERB}\alpha^{ni_{5,Rorc}}} - k_{m,Rorc}Rorc\end{aligned}$$

$$\begin{aligned}\frac{d\text{PER1}}{dt} = &t_{Per1} * Per1 - a_{\text{PER1,CRY1}} * \text{PER1} * \text{CRY1} \\ &- a_{\text{PER1,CRY2}} * \text{PER1} * \text{CRY2} + d_{\text{PER1/CRY1}} * \text{PER1/CRY1} \\ &+ d_{\text{PER1/CRY2}} * \text{PER1/CRY2} - k_{p,\text{PER1}} * \text{PER1}\end{aligned} \tag{9.9}$$

$$\begin{aligned}\frac{d\text{PER2}}{dt} = &t_{Per2} * Per2 - a_{\text{PER2,CRY1}} * \text{PER2} * \text{CRY1} \\ &- a_{\text{PER2,CRY2}} * \text{PER2} * \text{CRY2} + d_{\text{PER2/CRY1}} * \text{PER2/CRY1} \\ &+ d_{\text{PER2/CRY2}} * \text{PER2/CRY2} - k_{p,\text{PER2}} * \text{PER2}\end{aligned} \tag{9.10}$$

$$\begin{aligned}\frac{d\text{CRY1}}{dt} = &t_{Cry1} * Cry1 - a_{\text{PER1,CRY1}} * \text{PER1} * \text{CRY1} \\ &- a_{\text{PER2,CRY1}} * \text{PER2} * \text{CRY1} + d_{\text{PER1/CRY1}} * \text{PER1/CRY1} \\ &+ d_{\text{PER2/CRY1}} * \text{PER2/CRY1} - k_{p,\text{CRY1}} * \text{CRY1}\end{aligned} \tag{9.11}$$

$$\frac{d\text{CRY2}}{dt} = t_{Cry2} * Cry2 - a_{\text{PER1,CRY2}} * \text{PER1} * \text{CRY2} - a_{\text{PER2,CRY2}} * \text{PER2} * \text{CRY2} + d_{\text{PER1/CRY2}} * \text{PER1/CRY2} + d_{\text{PER2/CRY2}} * \text{PER2/CRY2} - k_{p,\text{CRY2}} * \text{CRY2} \tag{9.12}$$

$$\frac{d\text{REV-ERB}\alpha}{dt} = t_{Rev\text{-}erb\alpha} * Rev\text{-}erb\alpha - k_{p,\text{REV-ERB}\alpha} * \text{REV-ERB}\alpha \tag{9.13}$$

$$\frac{d\text{CLK}}{dt} = t_{Clk} * Clk - a_{\text{CLK,BMAL1}} * \text{CLK} * \text{BMAL1} + d_{\text{CLK/BMAL1}} * \text{CLK/BMAL1} - k_{p,\text{CLK}} * \text{CLK} \tag{9.14}$$

$$\frac{d\text{BMAL1}}{dt} = t_{Bmal1} * Bmal1 - a_{\text{CLK,BMAL1}} * \text{CLK} * \text{BMAL1} + d_{\text{CLK/BMAL1}} * \text{CLK/BMAL1} - k_{p,\text{BMAL1}} * \text{BMAL1} \tag{9.15}$$

$$\frac{d\text{RORc}}{dt} = t_{Rorc} * Rorc - k_{p,\text{RORc}} * \text{RORc} \tag{9.16}$$

$$\frac{d\text{PER1/CRY1}}{dt} = a_{\text{PER1,CRY1}} * \text{PER1} * \text{CRY1} - d_{\text{PER1/CRY1}} * \text{PER1/CRY1} \tag{9.17}$$

$$\frac{d\text{PER2/CRY1}}{dt} = a_{\text{PER2,CRY1}} * \text{PER2} * \text{CRY1} - d_{\text{PER2/CRY1}} * \text{PER2/CRY1} \tag{9.18}$$

$$\frac{d\text{PER1/CRY2}}{dt} = a_{\text{PER1,CRY2}} * \text{PER1} * \text{CRY2} - d_{\text{PER1/CRY2}} * \text{PER1/CRY2} \tag{9.19}$$

$$\frac{d\text{PER2/CRY2}}{dt} = a_{\text{PER2,CRY2}} * \text{PER2} * \text{CRY2} - d_{\text{PER2/CRY2}} * \text{PER2/CRY2} \tag{9.20}$$

$$\frac{d\text{CLK/BMAL1}}{dt} = a_{\text{CLK,BMAL1}} * \text{CLK} * \text{BMAL1} - d_{\text{CLK/BMAL1}} * \text{CLK/BMAL1} \tag{9.21}$$

9.2 Parameters of numerical simulations

Our choice of parameter values are as follows:

$V_{0,Per1}$=0.000001, $V_{1,Per1}$=3.0, $V_{0,Per2}$=0.09, $V_{1,Per2}$=3.29, $V_{0,Cry1}$=0.26,
$V_{1,Cry1}$=2.44, $V_{2,Cry1}$=2.89, $V_{0,Cry2}$=1.29, $V_{1,Cry2}$=2.72, $V_{2,Cry2}$=0.1,
$V_{1,Rev\text{-}erb\alpha}$=11.06, $V_{0,Clk}$=3.98, $V_{1,Clk}$=3.36, $V_{0,Bmal1}$=1.98, $V_{1,Bmal1}$=4.12,
$V_{0,Rorc}$=0.06, $V_{1,Rorc}$=3.55, $V_{2,Rorc}$=0.46,

$na_{1,Per1}$=2.0, $ni_{1,Per1}$=2.0, $ni_{2,Per1}$=1.0, $ni_{3,Per1}$=2.0, $ni_{4,Per1}$=4.0,
$na_{1,Per2}$=10.0, $ni_{1,Per2}$=1.0, $ni_{2,Per2}$=1.0, $ni_{3,Per2}$=9.0, $ni_{4,Per2}$=8.0,
$na_{1,Cry1}$=4.91, $na_{2,Cry1}$=3.01, $ni_{1,Cry1}$=1.0, $ni_{2,Cry1}$=1.0, $ni_{3,Cry1}$=6.0,
$ni_{4,Cry1}$=4.0, $ni_{5,Cry1}$=2.24, $na_{1,Cry2}$=4.39, $na_{2,Cry2}$=4.43, $ni_{1,Cry2}$=1.0,
$ni_{2,Cry2}$=1.0, $ni_{3,Cry2}$=4.0, $ni_{4,Cry2}$=8.0, $ni_{5,Cry2}$=1.75, $na_{1,Rev\text{-}erb\alpha}$=4.40, $ni_{1,Rev\text{-}erb\alpha}$=0.15,
$ni_{2,Rev\text{-}erb\alpha}$=0.3, $ni_{3,Rev\text{-}erb\alpha}$=7.0, $ni_{4,Rev\text{-}erb\alpha}$=7.0,
$na_{1,Clk}$=3.50, $ni_{1,Clk}$=1.96, $na_{1,Bmal1}$=4.13, $ni_{1,Bmal1}$=0.02, $na_{1,Rorc}$=1.57,
$na_{2,Rorc}$=0.56, $ni_{1,Rorc}$=1.0, $ni_{2,Rorc}$=1.0, $ni_{3,Rorc}$=7.0, $ni_{4,Rorc}$=7.0,
$ni_{5,Rorc}$=4.33,

$KA_{1,Per1}$=1.98, $KI_{1,Per1}$=1.07, $KI_{2,Per1}$=3.96, $KI_{3,Per1}$=1.68, $KI_{4,Per1}$=3.11,
$KA_{1,Per2}$=1.90, $KI_{1,Per2}$=4.51, $KI_{2,Per2}$=2.98, $KI_{3,Per2}$=2.24, $KI_{4,Per2}$=3.31,
$KA_{1,Cry1}$=1.46, $KA_{2,Cry1}$=3.76, $KI_{1,Cry1}$=0.03, $KI_{2,Cry1}$=0.77, $KI_{3,Cry1}$=3.59,
$KI_{4,Cry1}$=3.44, $KI_{5,Cry1}$=2.82, $KA_{1,Cry2}$=0.69, $KA_{2,Cry2}$=2.96, $KI_{1,Cry2}$=4.63,
$KI_{2,Cry2}$=2.95, $KI_{3,Cry2}$=3.57, $KI_{4,Cry2}$=2.75, $KI_{5,Cry2}$=3.97, $KA_{1,Rev\text{-}erb\alpha}$=3.15,
$KI_{1,Rev\text{-}erb\alpha}$=3.56, $KI_{2,Rev\text{-}erb\alpha}$=3.62, $KI_{3,Rev\text{-}erb\alpha}$=4.71, $KI_{4,Rev\text{-}erb\alpha}$=1.23,
$KA_{1,Clk}$=1.59, $KI_{1,Clk}$=0.83, $KA_{1,Bmal1}$=2.59, $KI_{1,Bmal1}$=2.47, $KA_{1,Rorc}$=4.30,
$KA_{2,Rorc}$=4.89, $KI_{1,Rorc}$=3.49, $KI_{2,Rorc}$=2.34, $KI_{3,Rorc}$=2.71, $KI_{4,Rorc}$=2.09,
$KI_{5,Rorc}$=3.36,

$k_{m,Per1}$=2.18, $k_{m,Per2}$=0.20, $k_{m,Cry1}$=0.22, $k_{m,Cry2}$=0.41, $k_{m,Rev\text{-}erb\alpha}$=0.60,
$k_{m,Clk}$=3.19, $k_{m,Bmal1}$=1.42, $k_{m,Rorc}$=1.50, $k_{p,\mathrm{PER1}}$=2.58, $k_{p,\mathrm{PER2}}$=3.0,
$k_{p,\mathrm{CRY1}}$=0.312, $k_{p,\mathrm{CRY2}}$=5.9, $k_{p,\mathrm{REV\text{-}ERB}\alpha}$=0.31, $k_{p,\mathrm{CLK}}$=1.52, $k_{p,\mathrm{BMAL1}}$=2.28,
$k_{p,\mathrm{RORc}}$=3.33,

t_{Per1}=3.05, t_{Per2}=2.38, t_{Cry1}=3.94, t_{Cry2}=1.69, $t_{Rev\text{-}erb\alpha}$=1.60, t_{Clk}=3.04,
t_{Bmal1}=4.00, t_{Rorc}=1.39,

$a_{\mathrm{PER1,CRY1}}$=3.57, $a_{\mathrm{PER1,CRY2}}$=3.12, $a_{\mathrm{PER2,CRY1}}$=3.81, $a_{\mathrm{PER2,CRY2}}$=4.0,

$a_{\mathrm{CLK,BMAL1}}$=1.98, $d_{\mathrm{PER1/CRY1}}$=1.32, $d_{\mathrm{PER1/CRY2}}$=1.85, $d_{\mathrm{PER2/CRY1}}$=1.37, $d_{\mathrm{PER2/CRY2}}$=2.42, $d_{\mathrm{CLK/BMAL1}}$=0.97.

We calculated the dynamics of the model by Euler time steps $\Delta t = 0.001$.

References

[Ak&al98] T. Akutsu, S. Kuhara, O. Maruyama, and S. Miyano, A system for identifying genetic networks from gene expression patterns produced by gene disruptions and overexpressions. Genome Informatics **9**, 151-160 (1998).

[Ara&al09] Z. Arai, W. Kalies, H. Kokubu, K. Mischaikow, H. Oka, and P. Pilarczyk. A database schema for the analysis of global dynamics of multiparameter systems. SIAM J. Appl. Dyn. Syst. **8**, 757-789 (2009).

[Arn98] L. Arnold. *Random Dynamical Systems.* Springer-Verlag Berlin, 1998.

[Arn73] V.I. Arnold. *Ordinary Differential Equations.* MIT Press Cambridge MA 1973.

[BaVi92] A.V. Babin and M.I. Vishik. *Attractors of Evolution Equations.* North Holland, Amsterdam, 1992.

[BaCh11] R. Barboza and G. Chen. On the global boundedness of the Chen system. Int. J. Bif. Chaos **21**, 3373-3385 (2011).

[Be&al04] V.N. Belykh, I.V. Belykh, and M. Hasler. Connection graph stability method for synchronized coupled chaotic systems. Physica D **195**, 159-187 (2004).

[Ch&al08] J. Chen, Y. Liu, S. Lu, B. O'Sullivan, and I. Razgon. A fixed-parameter algorithm for the directed feedback vertex set problem. J. ACM **55**, 21:1-19 (2008).

[ChVi02] V.V. Chepyzhov and M.I. Vishik. *Attractors for Equations of Mathematical Physics.* Coll. Pub. AMS **49**, Providence RI 2002.

[Co&al89] P. Constantin, C. Foias, B. Nicolaenko, and R. Temam. *Integral manifolds and inertial manifolds for dissipative partial differential equations.* Appl. Math. Sciences **70**, Springer-Verlag New York 1989. Colloq. AMS, Providence, 2002.

[Ed&al94] A. Eden, C. Foias, B. Nicolaenko, and R. Temam. *Exponential Attractors for Dissipative Evolution Equations.* Wiley Chichester 1994.

[FoTe84] C. Foias and R. Temam. Determination of the solutions of the Navier-Stokes equations by a set of nodal values. Math. Comput. **43**, 117-133 (1984).

[FoTi91] C. Foias and E.S. Titi. Determining nodes, finite differences schemes and inertial manifolds. Nonlinearity **4**, 135-153 (1991).

[Go&al10] M. Golubitsky, D. Romano, and Y. Wang. Network periodic solutions: full oscillation and rigid synchrony. Nonlinearity **23**, 3227-3243 (2010).

[Ha88] J.K. Hale. *Asymptotic Behavior of Dissipative Systems*. Math. Surv. **25**, AMS Pub. Providence 1988.

[Ha&al02] J.K. Hale, L.T. Magalhães, and W.M. Oliva. *Dynamics in Infinite Dimensions.* Springer-Verlag New York 2002.

[HaRa03] J.K. Hale and G. Raugel. Regularity, determining modes and Galerkin methods. J. Math. Pures Appl., IX. **82**, 1075-1136 (2003).

[Im&al06] K. S. Imai, M. Levine, N. Satoh, and Y. Satou, Regulatory Blueprint for a Chordate Embryo. *Science* **312**, 1183-1187 (2006).

[Jo11] R. Joly. Observation and inverse problems in coupled cell networks. Nonlinearity **25**, 657-676 (2012).

[Ka75] R.M. Karp. Reducibility among combinatorial problems. Kibernet Sb. **12**, 16–83 (1975).

[KlRa11] P.E. Kloeden and M. Rasmussen. *Nonautonomous Dynamical Systems.* Math. Surv **176**, AMS Pub. Providence 2011.

[La72] O.A. Ladyzhenskaya. Dynamical system generated by the Navier-Stokes equations. Sov. Phys., Dokl. **17**, 647-649 (1972); translation from Dokl. Akad. Nauk SSSR **205**, 318-320 (1972).

[La91] O.A. Ladyzhenskaya. *Attractors for Semigroups and Evolution Equations*. Cambridge University Press 1991.

[Lo63] E.N. Lorenz. Deterministic nonperiodic flow. J. Atmos. Sci. **20**, 130-141 (1963).

[MPSe87] J. Mallet-Paret and G.R. Sell. The principle of spatial averaging and inertial manifolds for reaction- diffusion equations. In: Nonlinear semigroups, partial differential equations and attractors, Proc. Symp., Washington/D.C. 1985, Lect. Notes Math. **1248**, 94-107 (1987).

[Mi09] H. P. Mirsky, A. C. Liu, D. K. Welsh, S. A. Kay, and F. J. Doyle III, A model of the cell-autonomous mammalian circadian clock. *Proc. Natl. Acad. Sci. USA* **106**, 11107-11112 (2009).

[Mi&al01] K. Mischaikow, M. Mrozek, and A. Szymczak. Chaos in the Lorenz equations: A computer assisted proof. III: Classical parameter values. J. Differ. Equations **169** 17-56 (2001).

[Mo08] A. Mochizuki. Structure of regulatory networks and diversity of gene expression patterns. *J. theor. Biol.* **250**, 307-321. (2008).

[Mo&al13] A. Mochizuki, G. Kurosawa, D. Saito, and B. Fiedler. Dynamics and control at feedback vertex sets. II: Monitoring the diversity of molecular activities in regulatory networks. Submitted, 2013.

[MoSa10] A. Mochizuki and D. Saito, Analyzing steady states of dynamics of bio-molecules from the structure of regulatory networks. *J. Theor. Biol.* **266**, 323-335 (2010).

[Oda05] K. Oda, Y. Matsuoka, A. Funahashi, and H. Kitano, A comprehensive pathway map of epidermal growth factor receptor signaling. *Mol. Syst. Biol.* **1**, 1-17 (2005).

[PeCa98] L.M. Pecora and T.L. Carroll. Master stability functions for synchronized coupled systems. Phys. Rev. Letters **80**, 2109-2112 (1998).

[Ra02] G. Raugel. Global attractors. In *Handbook of Dynamical Systems, Vol. 2.* B. Fiedler (ed.), Elsevier, Amsterdam, 2002, 885–982.

[SeYo02] G.R. Sell and Y. You. *Dynamics of Evolutionary Equations.* Springer-Verlag, New York 2002.

[Sp82] C. Sparrow. *The Lorenz equations: bifurcations, chaos, and strange attractors.* Appl. Math. Sciences **41**. Springer-Verlag Berlin 1982.

[Ta10] F. Takens. Reconstruction theory and nonlinear time series analysis. In: H. Broer et al. (eds.), *Handbook of Dynamical Systems* **3**. Elsevier Amsterdam, 345-377 (2010).

[Te88] R. Temam. *Infinite-Dimensional Dynamical Systems in Mechanics and Physics*. Springer-Verlag New York 1988.

[Tu02] W. Tucker. A rigorous ODE solver and Smale's 14th problem. Found. Comput. Math. **2**, No. 1, 53-117 (2002).